Arabian Journal of Chemistry (2019) 12, 908–931

King Saud University

Arabian Journal of Chemistry

www.ksu.edu.sa
www.sciencedirect.com

REVIEW

Nanoparticles: Properties, applications and toxicities

Ibrahim Khan [a,*], Khalid Saeed [b], Idrees Khan [c]

[a] Center of Research Excellence in Nanotechnology (CENT), King Fahd University of Petroleum and Minerals (KFUPM), Saudi Arabia
[b] Department of Chemistry, Bacha Khan University, Charsadda, Pakistan
[c] Department of Chemistry, University of Malakand, Chakdara, Pakistan

Received 18 March 2017; accepted 10 May 2017
Available online 18 May 2017

KEYWORDS

Nanoparticles;
Fullerenes;
Optical;
Plasmonic;
Toxicity

Abstract This review is provided a detailed overview of the synthesis, properties and applications of nanoparticles (NPs) exist in different forms. NPs are tiny materials having size ranges from 1 to 100 nm. They can be classified into different classes based on their properties, shapes or sizes. The different groups include fullerenes, metal NPs, ceramic NPs, and polymeric NPs. NPs possess unique physical and chemical properties due to their high surface area and nanoscale size. Their optical properties are reported to be dependent on the size, which imparts different colors due to absorption in the visible region. Their reactivity, toughness and other properties are also dependent on their unique size, shape and structure. Due to these characteristics, they are suitable candidates for various commercial and domestic applications, which include catalysis, imaging, medical applications, energy-based research, and environmental applications. Heavy metal NPs of lead, mercury and tin are reported to be so rigid and stable that their degradation is not easily achievable, which can lead to many environmental toxicities.

Contents

* Corresponding author.
E-mail address: ebraheem.chemist@gmail.com (I. Khan).
Peer review under responsibility of King Saud University.

Production and hosting by Elsevier

http://dx.doi.org/10.1016/j.arabjc.2017.05.011

1. Introduction

Nanotechnology is a known field of research since last century. Since "nanotechnology" was presented by Nobel laureate Richard P. Feynman during his well famous 1959 lecture "*There's Plenty of Room at the Bottom*" (Feynman, 1960), there have been made various revolutionary developments in the field of nanotechnology. Nanotechnology produced materials of various types at nanoscale level. Nanoparticles (NPs) are wide class of materials that include particulate substances, which have one dimension less than 100 nm at least (Laurent et al., 2010). Depending on the overall shape these materials can be 0D, 1D, 2D or 3D (Tiwari et al., 2012). The importance of these materials realized when researchers found that size can influence the physiochemical properties of a substance e.g. the optical properties. A 20-nm gold (Au), platinum (Pt), silver (Ag), and palladium (Pd) NPs have characteristic wine red color, yellowish gray, black and dark black colors, respectively. Fig. 1 shows an example of this illustration, in which Au NPs synthesized with different sizes. These NPs showed characteristic colors and properties with the variation of size and shape, which can be utilized in bioimaging applications (Dreaden et al., 2012). As Fig. 1 indicates, the color of the solution changes due to variation in aspect ratio, nanoshell thickness and % gold concentration. The alteration of any of the above discussed factor influences the absorption properties of the NPs and hence different absorption colors are observed.

NPs are not simple molecules itself and therefore composed of three layers i.e. (a) The surface layer, which may be functionalized with a variety of small molecules, metal ions, surfactants and polymers. (b) The shell layer, which is chemically different material from the core in all aspects, and (c) The core, which is essentially the central portion of the NP and usually refers the NP itself (Shin et al., 2016). Owing to such exceptional characteristics, these materials got immense interest of researchers in multidisciplinary fields. Fig. 2 shows scanning electron microscopy (SEM) and transmittance electron microscope (TEM) images of mesoporous and nonporous methacrylate-functionalized silica (MA-SiO_2). Mesoporousity imparts additional characteristics in NPs. The NPs can be employed for drug delivery (Lee et al., 2011), chemical and biological sensing (Barrak et al., 2016), gas sensing (Mansha et al., 2016; Rawal and Kaur, 2013; Ullah et al., 2017), CO_2 capturing (Ganesh et al., 2017; Ramacharyulu et al., 2015) and other related applications (Shaalan et al., 2016).

In this review article, we provide a general overview on the different types, synthesis methods, characterizations, properties and applications of NPs. The last section is also provided with the future aspects and recommendations.

2. Classification of NPs

NPs are broadly divided into various categories depending on their morphology, size and chemical properties. Based on physical and chemical characteristics, some of the well-known classes of NPs are given as below.

2.1. Carbon-based NPs

Fullerenes and carbon nanotubes (CNTs) represent two major classes of carbon-based NPs. Fullerenes contain nanomaterial that are made of globular hollow cage such as allotropic forms of carbon. They have created noteworthy commercial interest

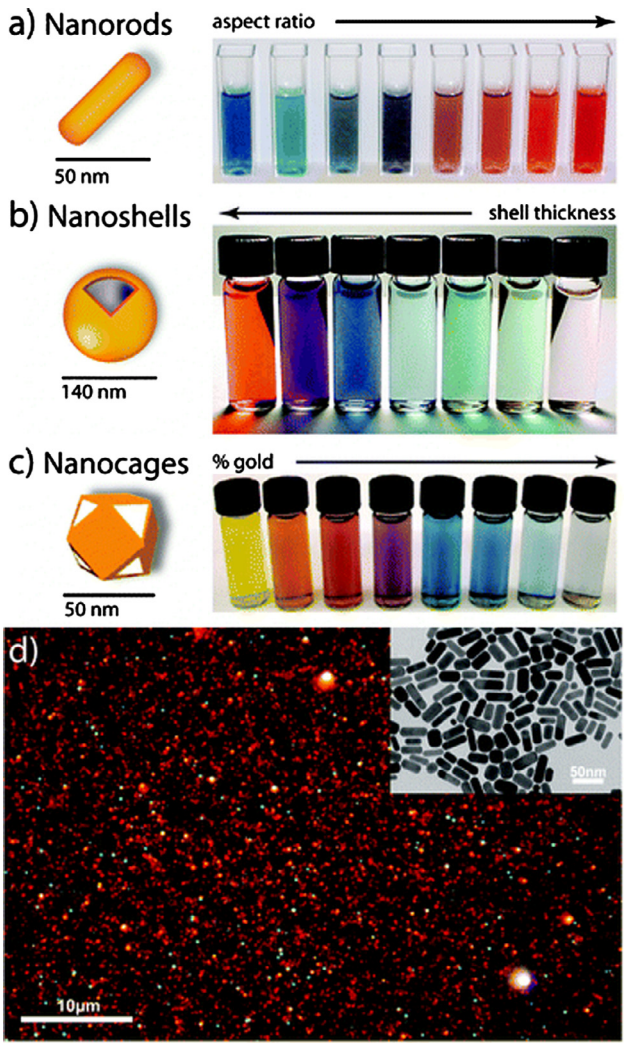

Figure 1 Color dependence of Au NPs on size and shape (Dreaden et al., 2012).

due to their electrical conductivity, high strength, structure, electron affinity, and versatility (Astefanei et al., 2015). These materials possess arranged pentagonal and hexagonal carbon units, while each carbon is sp^2 hybridized. Fig. 3 shows some of the well-known fullerenes consisting of C_{60} and C_{70} with the diameter of 7.114 and 7.648 nm, respectively.

CNTs are elongated, tubular structure, 1–2 nm in diameter (Ibrahim, 2013). These can be predicted as metallic or semiconducting reliant on their diameter telicity (Aqel et al., 2012). These are structurally resembling to graphite sheet rolling upon itself (Fig. 4). The rolled sheets can be single, double or many walls and therefore they named as single-walled (SWNTs), double-walled (DWNTs) or multi-walled carbon nanotubes (MWNTs), respectively. They are widely synthesized by deposition of carbon precursors especially the atomic carbons, vaporized from graphite by laser or by electric arc on to metal particles. Lately, they have been synthesized via chemical vapor deposition (CVD) technique (Elliott et al., 2013). Due to their unique physical, chemical and mechanical characteristics, these materials are not only used in pristine form but also in nanocomposites for many commercial applications such as fillers (Saeed and Khan, 2016, 2014), efficient gas adsorbents for environmental remediation (Ngoy et al., 2014), and as support medium for different inorganic and organic catalysts (Mabena et al., 2011).

2.2. Metal NPs

Metal NPs are purely made of the metals precursors. Due to well-known localized surface plasmon resonance (LSPR) characteristics, these NPs possess unique optoelectrical properties. NPs of the alkali and noble metals i.e. Cu, Ag and Au have a broad absorption band in the visible zone of the electromagnetic solar spectrum. The facet, size and shape controlled synthesis of metal NPs is important in present day cutting-edge materials (Dreaden et al., 2012). Due to their advanced optical properties, metal NPs find applications in many research areas. Gold NPs coating is widely used for the sampling of SEM, to enhance the electronic stream, which helps in obtaining high quality SEM images (Fig. 1). There are many other applications, which are deeply discussed in applications section of this review.

2.3. Ceramics NPs

Ceramics NPs are inorganic nonmetallic solids, synthesized via heat and successive cooling. They can be found in amorphous, polycrystalline, dense, porous or hollow forms (Sigmund et al., 2006). Therefore, these NPs are getting great attention of researchers due to their use in applications such as catalysis, photocatalysis, photodegradation of dyes, and imaging applications. (Thomas et al., 2015).

2.4. Semiconductor NPs

Semiconductor materials possess properties between metals and nonmetals and therefore they found various applications in the literature due to this property (Ali et al., 2017; Khan et al., 2017a). Semiconductor NPs possess wide bandgaps and therefore showed significant alteration in their properties with bandgap tuning. Therefore, they are very important materials in photocatalysis, photo optics and electronic devices (Sun, 2000). As an example, variety of semiconductor NPs are found exceptionally efficient in water splitting applications, due to their suitable bandgap and bandedge positions (Hisatomi et al., 2014).

2.5. Polymeric NPs

These are normally organic based NPs and in the literature a special term polymer nanoparticle (PNP) collective used for it. They are mostly nanospheres or nanocapsular shaped (Mansha et al., 2017). The former are matrix particles whose overall mass is generally solid and the other molecules are adsorbed at the outer boundary of the spherical surface. In the latter case the solid mass is encapsulated within the particle completely (Rao and Geckeler, 2011). The PNPs are readily functionalize and thus find bundles of applications in the literature (Abd Ellah and Abouelmagd, 2016; Abouelmagd et al., 2016).

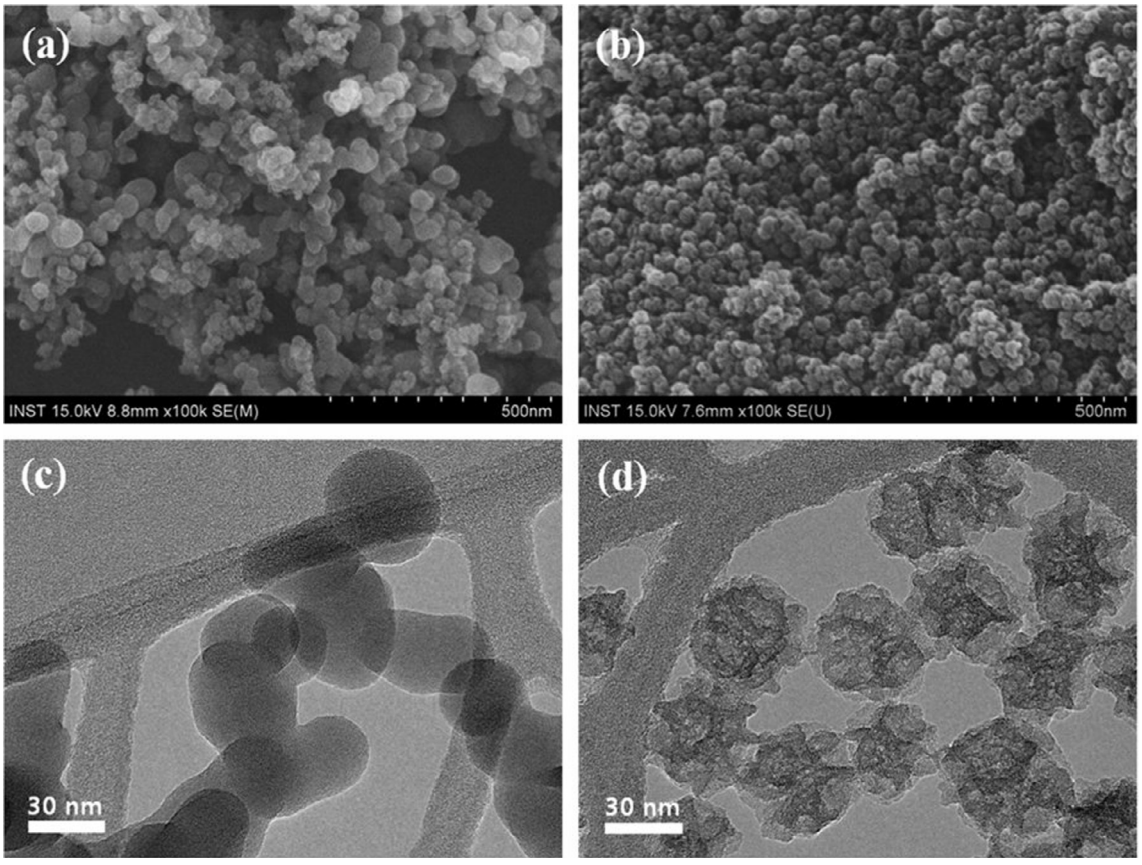

Figure 2 FE-SEM micrographs of (a) nonporous MA-SiO_2 NPs, (b) mesoporous MA-SiO_2 NPs. TEM images of (c) nonporous MA-SiO_2 NPs and (d) mesoporous MA-SiO_2 NPs (Lee et al., 2011).

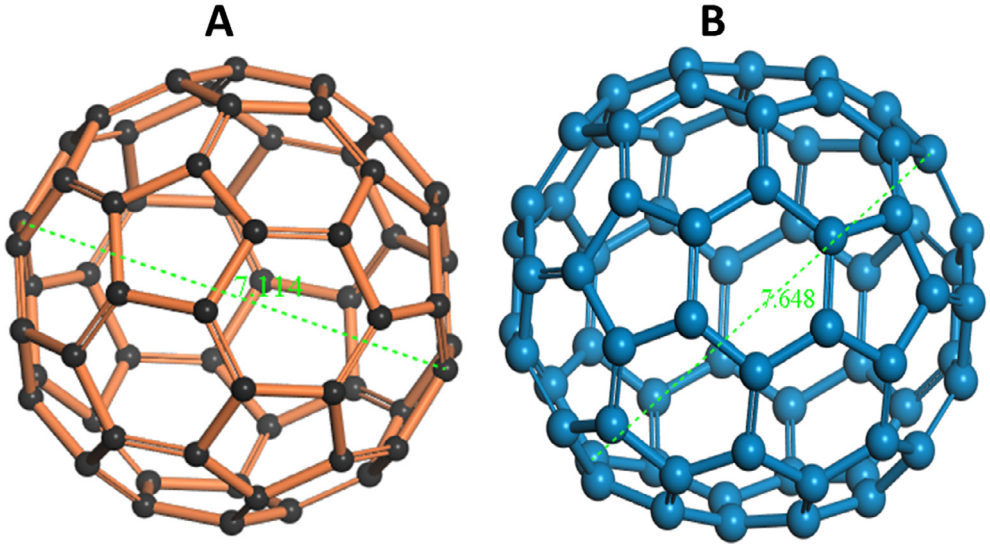

Figure 3 Different form of Fullerenes/buck balls (A) C_{60} and (B) C_{70}.

2.6. Lipid-based NPs

These NPs contain lipid moieties and effectively using in many biomedical applications. Generally, a lipid NP is characteristically spherical with diameter ranging from 10 to 1000 nm. Like polymeric NPs, lipid NPs possess a solid core made of lipid and a matrix contains soluble lipophilic molecules. Surfactants or emulsifiers stabilized the external core of these NPs (Rawat

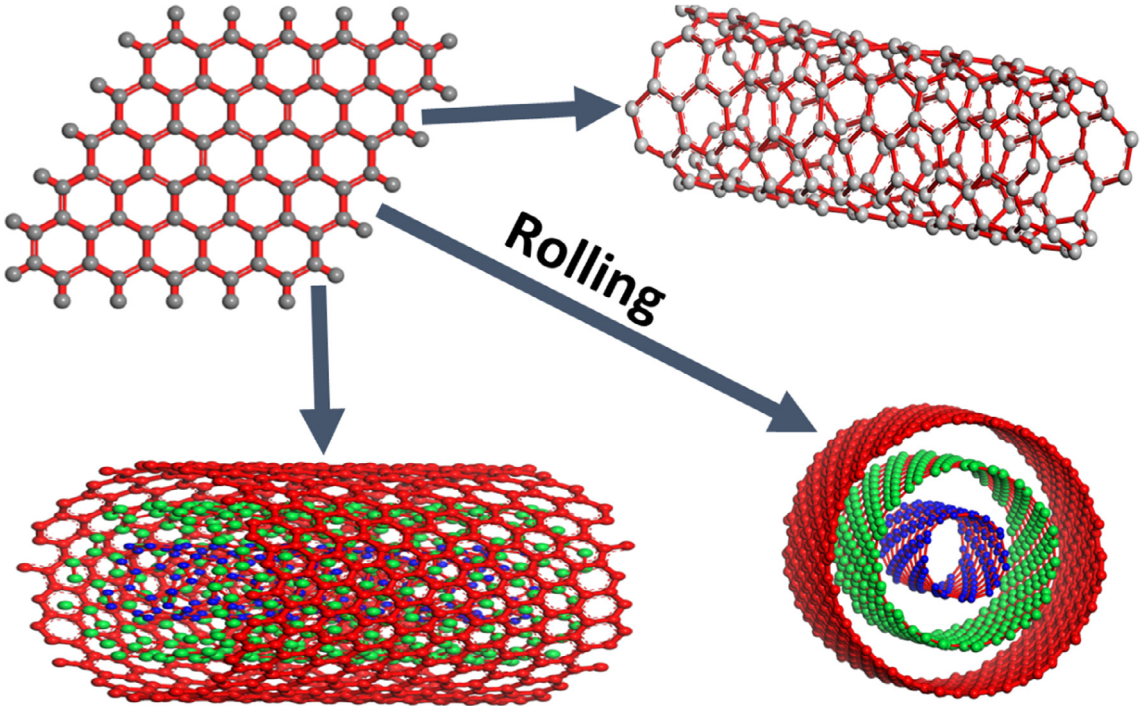

Figure 4 Rolling of graphite layer into single-walled and multi-walled CNTs.

et al., 2011). Lipid nanotechnology (Mashaghi et al., 2013) is a special field, which focus the designing and synthesis of lipid NPs for various applications such as drug carriers and delivery (Puri et al., 2009) and RNA release in cancer therapy (Gujrati et al., 2014).

3. Synthesis of nanoparticles

Various methods can be employed for the synthesis of NPs, but these methods are broadly divided into two main classes i.e. (1) Bottom-up approach and (2) Top-down approach (Wang and Xia, 2004) as shown in Scheme 1 (Iravani, 2011). These approaches further divide into various subclasses based on the operation, reaction condition and adopted protocols.

3.1. Top-down syntheses

In this method, destructive approach is employed. Starting from larger molecule, which decomposed into smaller units and then these units are converted into suitable NPs. Examples

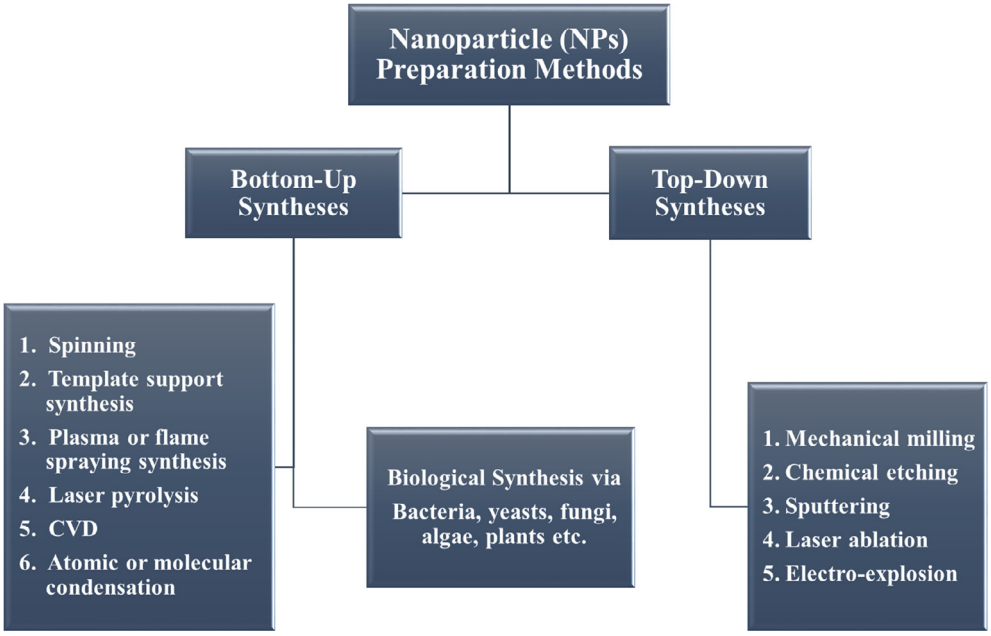

Scheme 1 Typical synthetic methods for NPs for the (a) top-down and (b) bottom-up approaches.

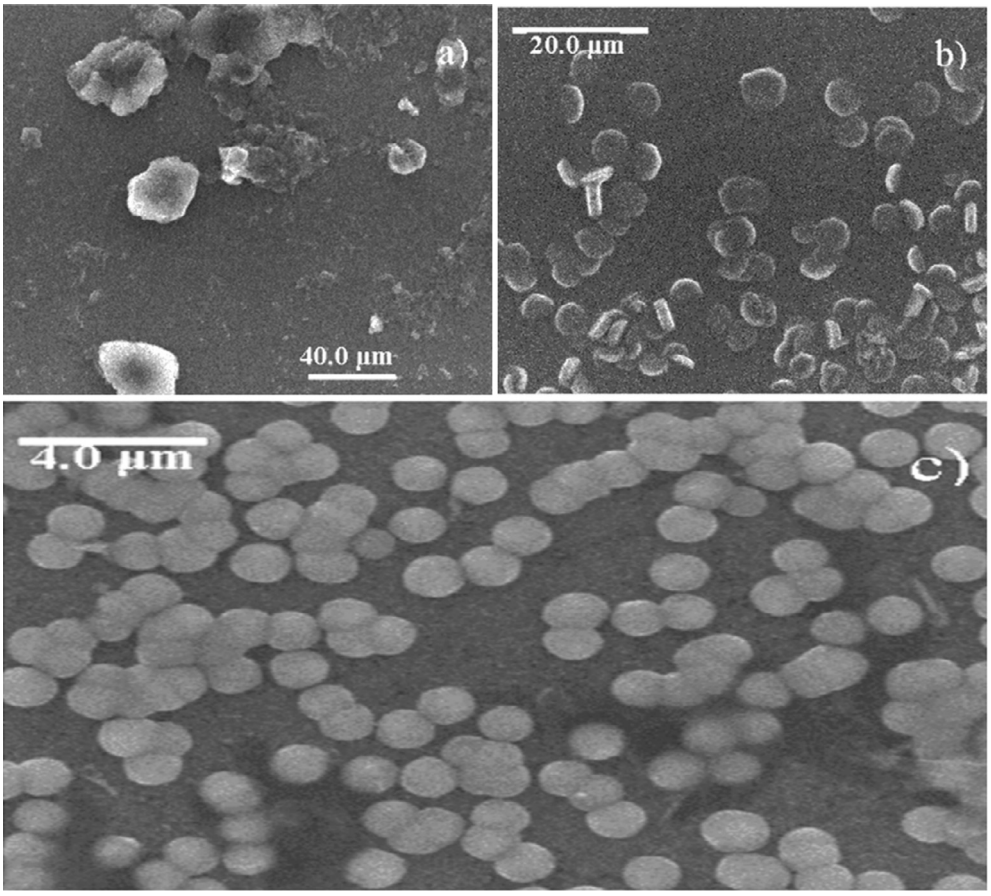

Figure 5 SEM images of (a) The untreated carbon black, (b) and (c) 10 min and 1 h ultrasonication in POM solution (Garrigue et al., 2004).

of this method are grinding/milling, CVD, physical vapor deposition (PVD) and other decomposition techniques (Iravani, 2011). This approach is used to synthesized coconut shell (CS) NPs. The milling method was employed for this purpose and the raw CS powders were finely milled for different interval of times, with the help of ceramic balls and a well-known planetary mill. They showed the effect of milling time on the overall size of the NPs through different characterization techniques. It was determined that with the time increases the NPs crystallite size decreases, as calculated by Scherer equation. They also realized that with each hour increment the brownish color faded away due to size decrease of the NPs. The SEM results were also in an agreement with the X-ray pattern, which also indicated the particle size decreases with time (Bello et al., 2015).

One study revealed the spherical magnetite NPs synthesis from natural iron oxide (Fe_2O_3) ore by top-down destructive approach with a particle size varies from ~20 to ~50 nm in the presence of organic oleic acid (Priyadarshana et al., 2015). A simple top-down route was employed to synthesize colloidal carbon spherical particles with control size. The synthesis technique was based on the continuous chemical adsorption of polyoxometalates (POM) on the carbon interfacial surface. Adsorption made the carbon black aggregates into relatively smaller spherical particles, with high dispersion capacity and narrow size distribution as shown in Fig. 5 (Garrigue et al., 2004). It also revealed from the micrographs, that the size of the carbon particles become smaller with sonication time. A series of transition-metal dichalcogenide nanodots (TMD-NDs) were synthesized by combination of grinding and sonication top-down techniques from their bulk crystals. It was revealed that almost all the TMD-NDs with sizes < 10 nm show an excellent dispersion due to narrow size distribution (Zhang et al., 2015). Lately, highly photoactive active Co_3O_4 NPs were prepared via top-down laser fragmentation, which is a top-down process. The powerful laser irradiations generate well-uniform NPs having good oxygen vacancies (Zhou et al., 2016). The average size of the Co_3O_4 was determined to be in the range of 5.8 nm $\pm$ 1.1 nm.

3.2. Bottom-up syntheses

This approach is employed in reverse as NPs are formed from relatively simpler substances, therefore this approach is also called building up approach. Examples of this case are sedimentation and reduction techniques. It includes sol gel, green synthesis, spinning, and biochemical synthesis. (Iravani, 2011). Mogilevsky et al. synthesized TiO_2 anatase NPs with graphene domains through this technique (Mogilevsky et al., 2014). They used alizarin and titanium isopropoxide precursors to synthesize the photoactive composite for photocatalytic degradation of methylene blue. Alizarin was selected as it offers strong binding capacity with TiO_2 through their axial

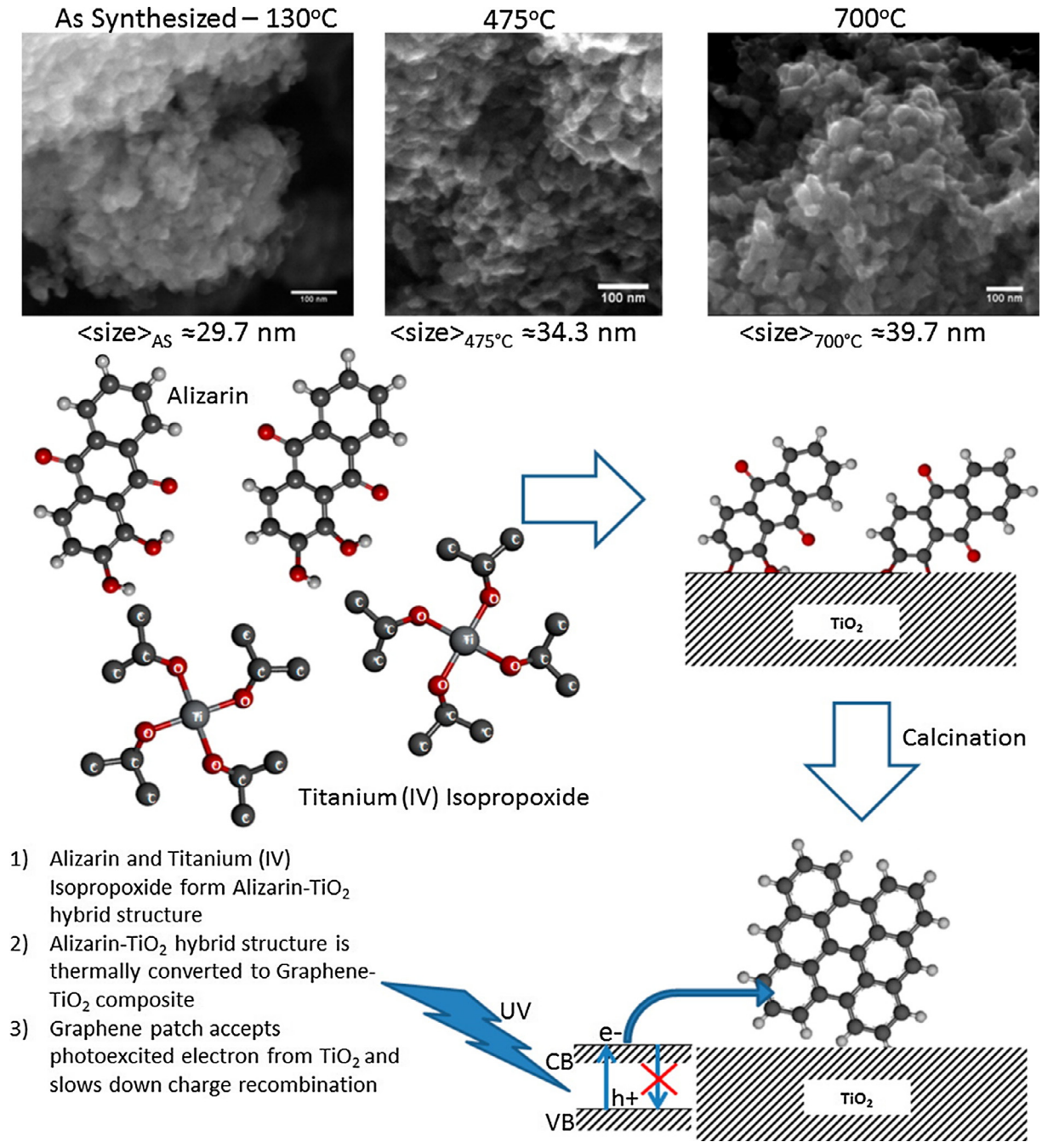

Scheme 2 Synthesis of TiO_2 via bottom-up technique. SEM images showing the TiO_2 NPs (Mogilevsky et al., 2014).

hydroxyl terminal groups. The anatase form was confirmed by XRD pattern. The SEM images taken for different samples with reaction scheme are provided in scheme 2. SEM indicates that with temperature elevation, the size of NPs also increases (Mogilevsky et al., 2014).

Well-uniform spherical shaped Au nanospheres with monocrystalline have been synthesized via laser irradiation top-down technique (Liu et al., 2015a, 2015b). Liu et al. selectively transform the octahedra morphology to spherical shape by controlling the laser treatment time and other reaction parameters. Fig. 6 provides the SEM and TEM of the prepared Au nanospheres, which showed average diameter of 75 ± 2.6 nm of Au nanospheres (red column Fig. 6e) and 72 ± 3.1 in edge length of Au octahedra per particle (blue column Fig. 6f).

More recently, solvent-exchange method is used to achieve limit sized low density lipoprotein (LDL) NPs for medical cancer drug delivery purpose by Needham et al. In this method nucleation is the bottom approach followed by growth which is the up approach. The LDL NPs were obtained without using phospholipid and possessed high hydrophobicity, which is essential for drug delivery applications (Needham et al., 2016).

The monodispersed spherical bismuth (Bi) NPs were synthesized by both top-down and bottom-up approaches

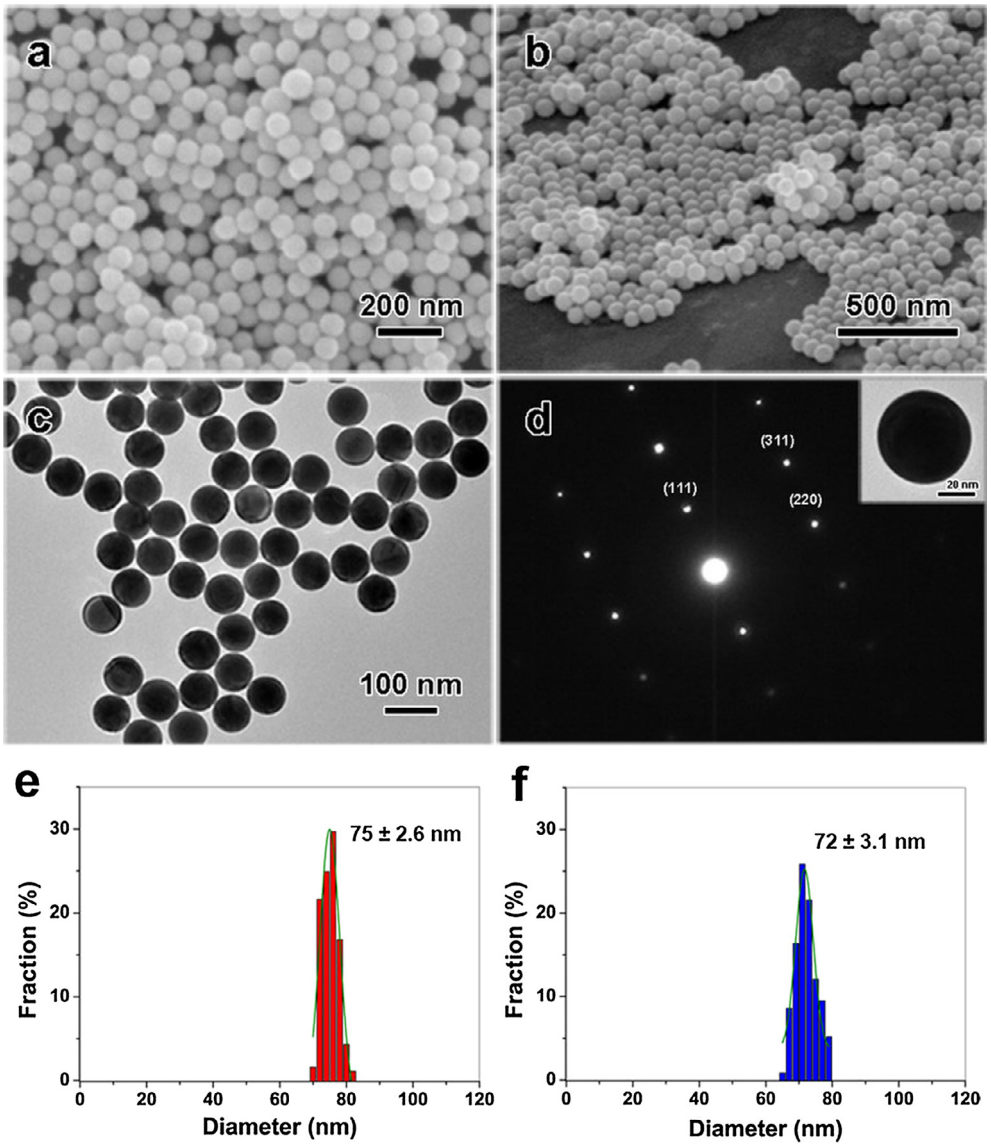

Figure 6 SEM for Au nanospheres (a) top view, (b) tilted view, (c) TEM image of Au nanospheres (d) SAED pattern (inset: TEM of single Au particle), (e) and (f) size distribution spectra of spherical and octahedral Au NPs (Liu et al., 2015a, 2015b).

(Wang and Xia, 2004). These NPs have excellent colloidal properties. In the bottom-up approach bismuth acetate was boiled within ethylene glycol, while in top-down approach the bismuth was converted into molten form and then the molten drop was emulsified within the boiled diethylene glycol to produce the NPs. The size of the NPs obtained by both methods was varied from 100 nm to 500 nm (Wang and Xia, 2004). The details of this study are provided in Scheme 3. Green and biogenic bottom-up synthesis attracting many researchers due to the feasibility and less toxic nature of processes. These processes are cost-effective and environmental friendly, where synthesis of NPs is accomplished via biological systems such as using plant extracts. Bacteria, yeast, fungi, *Aloe vera*, tamarind and even human cells are used for the synthesis of NPs. Au NPs have been synthesis from the biomass of wheat and oat (Parveen et al., 2016) and using the microorganism and plant extracts as reducing agent (Ahmed et al., 2016). Table 1 provides the merits and demerits of various top-down and bottom-up techniques with general remarks (Biswas et al., 2012).

4. Characterization of NPs

Different characterization techniques have been practiced for the analysis of various physicochemical properties of NPs. These include techniques such as X-ray diffraction (XRD), X-ray photoelectron spectroscopy (XPS), infrared (IR), SEM, TEM, Brunauer–Emmett–Teller (BET), and particle size analysis.

4.1. Morphological characterizations

The morphological features of NPs always attain great interest since morphology always influences most of the properties of the NPs. There are different characterization techniques for

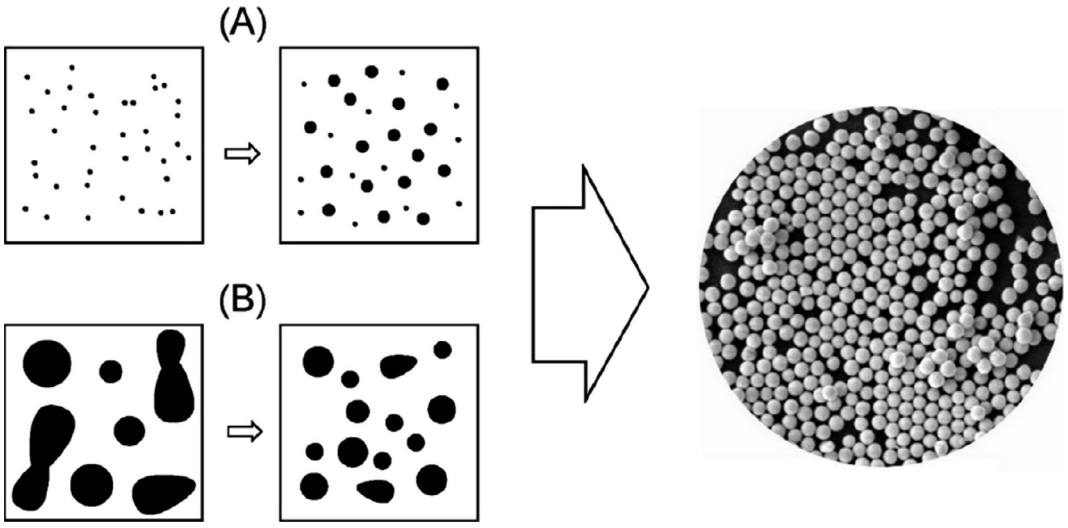

Scheme 3 (A) Bottom-up approach: A molecular precursor is disintegrated to simpler metal atoms that grow into colloids. (B) Top-down approach: Large drops of a metal broken into smaller drops (Wang and Xia, 2004).

morphological studies, but microscopic techniques such as polarized optical microscopy (POM), SEM and TEM are the most important of these.

SEM technique is based on electron scanning principle, and it provides all available information about the NPs at nanoscale level. Wide literature is available, where people used this technique to study not only the morphology of their nanomaterials, but also the dispersion of NPs in the bulk or matrix. The dispersion of SWNTs in the polymer matrix poly(butylene) terephthalate (PBT) and nylon-6 revealed through this technique (Saeed and Khan, 2016, 2014). The same group also provides POM study of their materials, which showed star-like spherulites of the formed materials, whose size was decreased with the incremental filling of SWNTs. The morphological features of ZnO modified metal organic frameworks (MOFs) were studied through SEM technique, which indicates the ZnO NPs dispersion and morphologies of MOFs at different reaction conditions (Fig. 7) (Mirzadeh and Akhbari, 2016).

Similarly, TEM is based on electron transmittance principle, so it can provide information of the bulk material from very low to higher magnification. The different morphologies of gold NPs are studied via this technique. Fig. 8 provides some TEM micrographs showing various morphologies of gold NPs, prepared via different methods (Khlebtsov and Dykman, 2011, 2010a, 2010b). TEM also provides essential information about two or more layer materials, such as the quadrupolar hollow shell structure of Co_3O_4 NPs observed through TEM. These NPs founded to be exceptionally active as anode in Li-ion batteries (Fig. 9). Porous multishell structure induces shorter Li^+ diffusion path length with adequate annulled space to buffer the volume expansion, good cycling performance, greater rate capacity, and specific capacity as well (Wang et al., 2013).

4.2. Structural characterizations

The structural characteristics are of the primary importance to study the composition and nature of bonding materials. It provides diverse information about the bulk properties of the subject material. XRD, energy dispersive X-ray (EDX), XPS, IR, Raman, BET, and Zieta size analyzer are the common techniques used to study structural properties of NPs.

XRD is one of the most important characterization techniques to reveal the structural properties of NPs. It gives enough information about the crystallinity and phase of NPs. It also provides rough idea about the particle size through Debye Scherer formula (Khan et al., 2017b, 2017c; Ullah et al., 2017). This technique worked well in both single and multiphase NPs identification (Emery et al., 2016). Nevertheless, in the case of smaller NPs having size less than hundreds of atoms, the acquisition and correct measurement of structural and other parameters may be difficult. Moreover, NPs having more amorphous characteristics with varied inter atomic lengths can influence the XRD diffractogram. In that case, proper comparison of the diffractograms of bimetallic NPs with those of the corresponding monometallic NPs and their physical mixtures is required to obtain accurate information. Comparison of computer simulated structural model of bimetallic NPs with observed XRD spectra is the best way to get good contrast (Ingham, 2015). EDX, which is normally fixed with field emission scanning electron miscopy (FE-SEM) or TEM device is widely used to know about the elemental composition with a rough idea of % wt. The electron beam focused over a single NP by SEM or TEM through the program functions, to acquire the insight information from the NP under observation. NP comprises of constituent elements and each of them emits characteristics energy X-rays by electron beam irradiation. The intensity of specific X-ray is directly proportional to the concentration of the explicit element in the particle. This technique is widely used by researchers to give support to SEM and other techniques for the confirmation of their elements in prepared materials (Avasare et al., 2015; Iqbal et al., 2016). The EDX technique used to determine the elemental composition of ultra-sonochemically synthesized pseudo-flower shaped $BiVO_4$ NPs (Khan et al., 2017b). Similarly, by utilizing similar technique the elemental confirmation and graphene impregnation of In_2O_3/graphene heterostructure NPs was carried out, which showed C, In and O as contribut-

Table 1 Top-down and bottom-up synthetic techniques with merits, demerits and general remarks (Biswas et al., 2012).

Top–down method	Merits	Demerits	General remarks
Optical lithography	Long-standing, established micro/nanofabrication tool especially for chip production, sufficient level of resolution at high throughputs	Tradeoff between resist process sensitivity and resolution, involves state-of-the-art expensive clean room based complex operations	The 193 nm lithography infrastructure already reached a certain level of maturity and sophistication, and the approach could be extended to extreme ultraviolet (EUV) sources to shrink the dimension. Also, future developments need to address the growing cost of a mask set
E-beam lithography	Popular in research environments, an extremely accurate method and effective nanofabrication tool for < 20 nm nanostructure fabrication with desired shape	Expensive, low throughput and a slow process (serial writing process), difficult for < 5 nm nanofabrication	E-beam lithography beats the diffraction limit of light, capable of making periodic nanostructure features. In the future, multiple electron beam approaches to lithography would be required to increase the throughput and degree of parallelism
Soft and nanoimprint lithography	Pattern transfer based simple, effective nanofabrication tool for fabricating ultra-small features (< 10 nm)	Difficult for large-scale production of densely packed nanostructures, also dependent on other lithography techniques to generate the template, and usually not cost-effective	Self-assembled nanostructures could be a viable solution to the problem of complex and costly template generation, and for templates of periodic patterns of < 10 nm
Block co-polymer lithography	A high-throughput, low-cost method, suitable for large-scale densely packed nanostructures, diverse shapes of nanostructures, including spheres, cylinders, lamellae possible to fabricate including parallel assembly	Difficult to make self-assembled nanopatterns with variable periodicity required for many functional applications, usually high defect densities in block copolymer self-assembled patterns	Use of triblock copolymers is promising to generate more exotic nanopattern geometries. Also, functionalization of parts of the block copolymer could be done to achieve hierarchy of nanopatterning in a single step nanofabrication process
Scanning probe lithography	High resolution chemical, molecular and mechanical nanopatterning capabilities, accurately controlled nanopatterns in resists for transfer to silicon, ability to manipulate big molecules and individual atoms	Limited for high throughput applications and manufacturing, an expensive process, particularly in the case of ultra-high-vacuum based scanning probe lithography	Scanning probe lithography can be leveraged for advanced bionanofabrication that involves fabrication of highly periodic biomolecular nanostructures
Bottom–up method	**Merits**	**Demerits**	**General remarks**
Atomic layer deposition	Allows digital thickness control to the atomic level precision by depositing one atomic layer at a time, pin-hole free nanostructured films over large areas, good reproducibility and adhesion due to the formation of chemical bonds at the first atomic layer	Usually a slow process, also an expensive method due to the involvement of vacuum components, difficult to deposit certain metals, multicomponent oxides, certain technologically important semiconductors (Si, Ge, etc.) in a cost-effective way	Although a slow process, it is not detrimental for the fabrication of future generation ultra-thin ICs. The stringent requirements for the metal barriers (pure; dense; conductive; conformal; thin) that are employed in modern Cu-based chips can be fulfilled by atomic layer deposition
Sol gel nanofabrication	A low-cost chemical synthesis process based method, fabrication of a wide variety of nanomaterials including multicomponent materials (glass, ceramic, film, fiber, composite materials)	Not easily scalable, usually difficult to control synthesis and the subsequent drying steps	A versatile nanofabrication method that can be made scalable with further advances in the synthesis steps
Molecular self-assembly	Allows self-assembly of deep molecular nanopatterns of width less than 20 nm and with the large pattern stretches, generates atomically precise nanosystems	Difficult to design and fabricate nanosystems unlike mechanically directed assembly	Molecular self-assembly of multiple materials may be an useful approach in developing multifunctional nanosystems and devices
Physical and chemical vapor-phase deposition	Versatile nanofabrication tools for fabrication of nanomaterials including complex multicomponent nanosystems (e.g. nanocomposites), controlled simultaneous deposition of several	Not cost-effective because of the expensive vacuum components, high-temperature process and toxic and corrosive gases particularly in the case of chemical vapor deposition	It provides unique opportunity of nanofabrication of highly complex nanostructures made of distinctly different materials with different properties that are not possible to

(*continued on next page*)

Table 1 (*continued*)

Bottom–up method	Merits	Demerits	General remarks
	materials including metal, ceramics, semiconductors, insulators and polymers, high purity nanofilms, a scalable process, possibility to deposit porous nanofilms		accomplish using most of the other nanofabrication techniques. New advances in chemical vapor deposition such as 'initiated chemical vapor deposition' (i-CVD) provide unprecedented opportunities of depositing polymers without reduction in the molecular weights
DNA-scaffolding	Allows high-precision assembling of nanoscale components into programmable arrangements with much smaller dimensions (less than 10 nm in half-pitch)	Many issues need to explore, such as novel unit and integration processes, compatibility with CMOS fabrication, line edge roughness, throughput and cost	Very early stage. Ultimate success depends on the willingness of the semiconductor industry in terms of need, infrastructural capital investment, yield and manufacturing cost

ing elements. This material was synthesized through conventional hydrothermal technique (Mansha et al., 2016).

XPS is considered to be the most sensitive technique and it is widely used to determine the exact elemental ratio and exact bonding nature of the elements in NPs materials. It is surface sensitive technique and can be used in depth profiling studies to know the overall composition and the compositional variation with depth. XPS is based on the basic spectroscopic principles and typical XPS spectrum is composed of the number of electrons on Y-axis plot versus the binding energy (eV) of the electrons on X-axis. Each element has their own fingerprint binding energy value and thus gives specific set of XPS peaks. The peaks correspond come from electronic configuration, e.g., 1s, 2s, 2p, and 3s. Lykhach et al. provide a depth electron transfer study through CeO_2 supported Pt NPs using XPS technique with support to others. They determined that per ten Pt atoms, only one electron is elated from the NPs to CeO_2 support (Lykhach et al., 2015). The depth profile analysis was provided to study the dispersion of boron NPs (10 nm size) during polyethylene glycol (PEG) functionalization. Ar^+ ions were used at 1.4 keV and 20 nm; depth surface etching was performed. It was revealed that the concentration of NPs increases from 2 to 5% with depth. This provided good evidence that boron NPs are dissolved effectively within the bulk of functionalized PEG (Oprea et al., 2015). In similar study coreshell Au/Ag showed similar behavior through XPS depth profiling. Wang et al. quantify the NPs coating with this technique through XPS and STEM spectroscopies by help of SESSA software (Wang et al., 2016).

Vibrational characterization of nanoparticles is normally studied via FT-IR and Raman spectroscopies. These techniques are the most developed and feasible as compared to other elemental analytical methods. The most important range for NPs is the fingerprint region, which provides signature information about the material. In one study, functionalization of Pt NPs (1.7 nm mean size) and its interaction with Alumina substrate studied via FT-IR and XPS technique. FT-IR confirms the functionalization as it showed the signature vibrational peaks of carboxylated C–O 2033 cm^{-1}, respectively in addition to a broader O–H peak at 3280 cm^{-1}. The degree of functionalization was revealed from the red shift values of FT-IR bands (Fig. 10) (Dablemont et al., 2008).

In another study, a series of 5 mol% Eu^{3+} – doped rare earth metal (RE) hafnium oxide $RE_2Hf_2O_7$ (where RE = Y, Pr, La, Gd, Lu and Er) (NPs) was synthesized by correlated techniques. FT-IR and Raman spectra analysis exhibited that the $La_2Hf_2O_7$:5%Eu^{3+} and $Pr_2Hf_2O_7$:5%Eu^{3+} possessed relatively ordered pyrochlore structure as compared to $RE_2Hf_2O_7$:5%Eu^{3+} compositions (RE = Y, Er, and Lu), which possess disordered fluorite structure. The stable structures were found thermodynamically stable until high temperature of 1500 °C. However, a disordered–ordered cause instability in the latter case, and thus thermodynamically unstable (Pokhrel et al., 2016).

More recently surface enhanced Raman spectroscopy (SERS) is evolving as vibrational conformational tool due to its signal enhanced capability via SPR phenomenon (Muehlethaler et al., 2016). One study reported SERS technique to study the vibrational properties with phonons modes in nanostructured and quantum dots NPS of TiO_2, ZnO and PbS. They concluded that the enhanced spectra can be attributed to the plasmonic resonances in semiconductor systems (Ma et al., 2011).

4.3. Particle size and surface area characterization

Different techniques can be used to estimate the size of the NPs. These include SEM, TEM, XRD, AFM, and dynamic light scattering (DLS). SEM, TEM, XRD and AFM can give better idea about the particle size (Kestens et al., 2016), but the zeta potential size analyzer/DLS can be used to find the NPs size at extremely low level. In one study Sikora et al. used DLS technique to investigate the size variation of silica NPs with absorption of proteins from serum. The results showed that size increased with acquisition of protein layer. However, in case of agglomeration and hydrophilicity, DLS might prove incapable of accurate measurement, so in that case we should rely on the high-resolution technique of differential centrifugal sedimentation (DCS) (Sikora et al., 2016). Beside DSC, nanoparticle tracking analysis (NTA) is relatively newer and special technique, which can be helpful in case of biological systems such as proteins, and DNA. In NTA method, we can visualize and analyze the NPs in liquids media that relates the Brownian motion rate to particle size. This technique allows us to find the size distribution profile of NPs with diameter ranging from 10 to 1000 nm in a liquid medium (Filipe et al., 2010). This technique produced some good results as

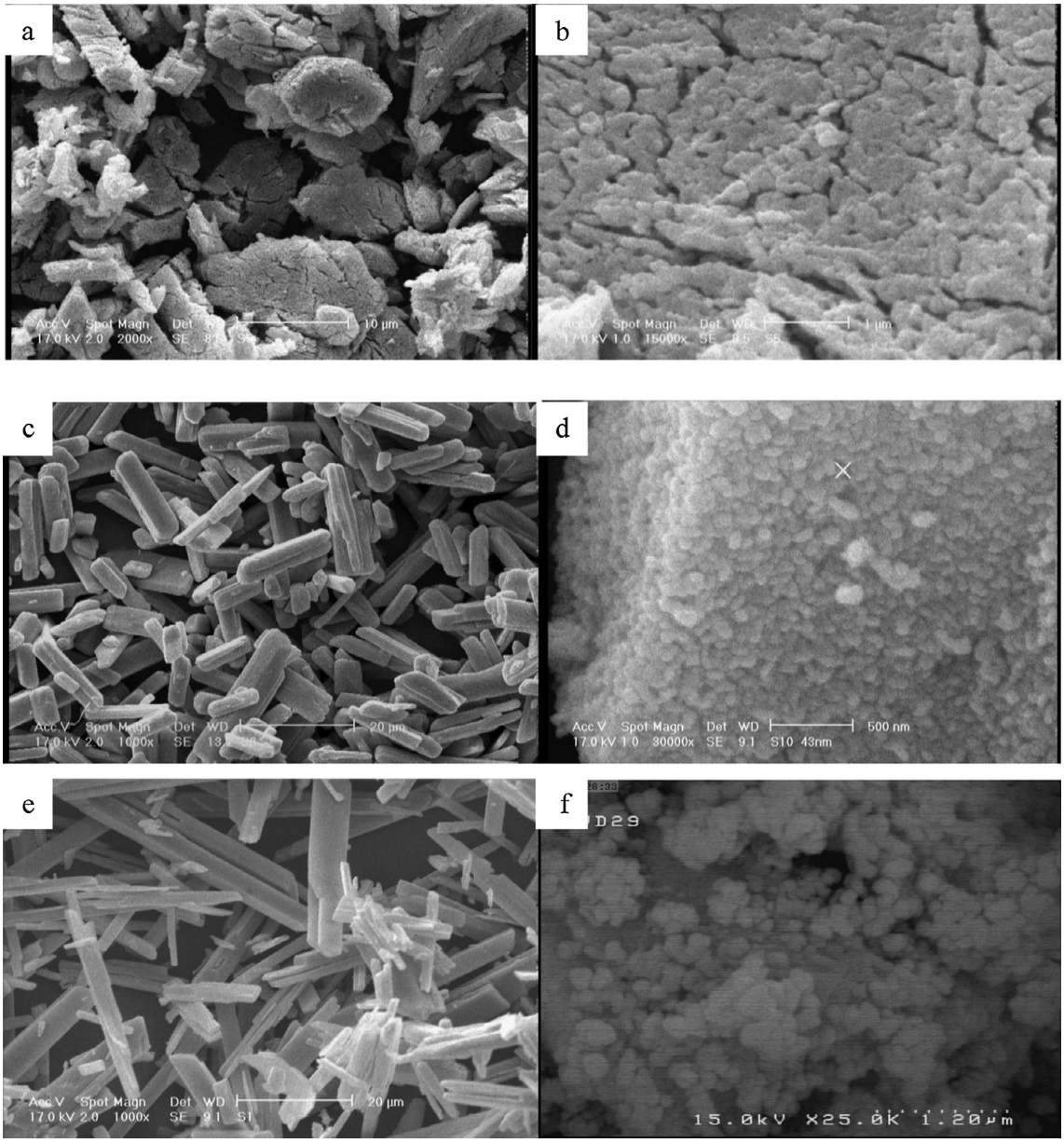

Figure 7 SEM images of ZnO modified MOFs at different temperatures (Mirzadeh and Akhbari, 2016).

compared to DLS and found to be very precise for sizing monodisperse as well as polydisperse samples, with substantially better peak resolution. Gross et al. detected the particle size and concentration of different sized NPs in suspensions of polymer and protein samples and provided an overview on the effect of experimental and data evaluation parameters (Gross et al., 2016).

Large surface area of nanomaterials offers great room for various applications and BET is the best technique to determine the surface area of NPs materials. This technique is based on adsorption and desorption principle and Brunauer–Emmett–Teller (BET) theorem. Normally nitrogen gas is used for this purpose. BET produces four types of isotherm specifically, which are labeled as Type-I, Type-II, Type-III and Type-IV (Fagerlund, 1973). The fresh $7Cu_3Ce$/ZSM-5 showed typical features of Type-I isotherm obtain from nitrogen adsorption/desorption. It was discovered that N_2 adsorption volume is progressively increased with relative pressure until certain limit signifying the availability of pores. The BET specific surface area for this material was 133–144 m^2/g, while the total pore volume was 0.112–0.185 cm^3/g. But after sulphidation process, the BET surface area reduced to 110 m^2/mg and the pore volume decreased to 0.096 cm^3/g, respectively (Liu et al., 2016).

4.4. Optical characterizations

Optical properties are of great concerned in photocatalytic applications and therefore, photo-chemists acquired good knowledge of this technique to reveal the mechanism of their photochemical processes. These characterizations are based on the famous beer-lambert law and basic light principles

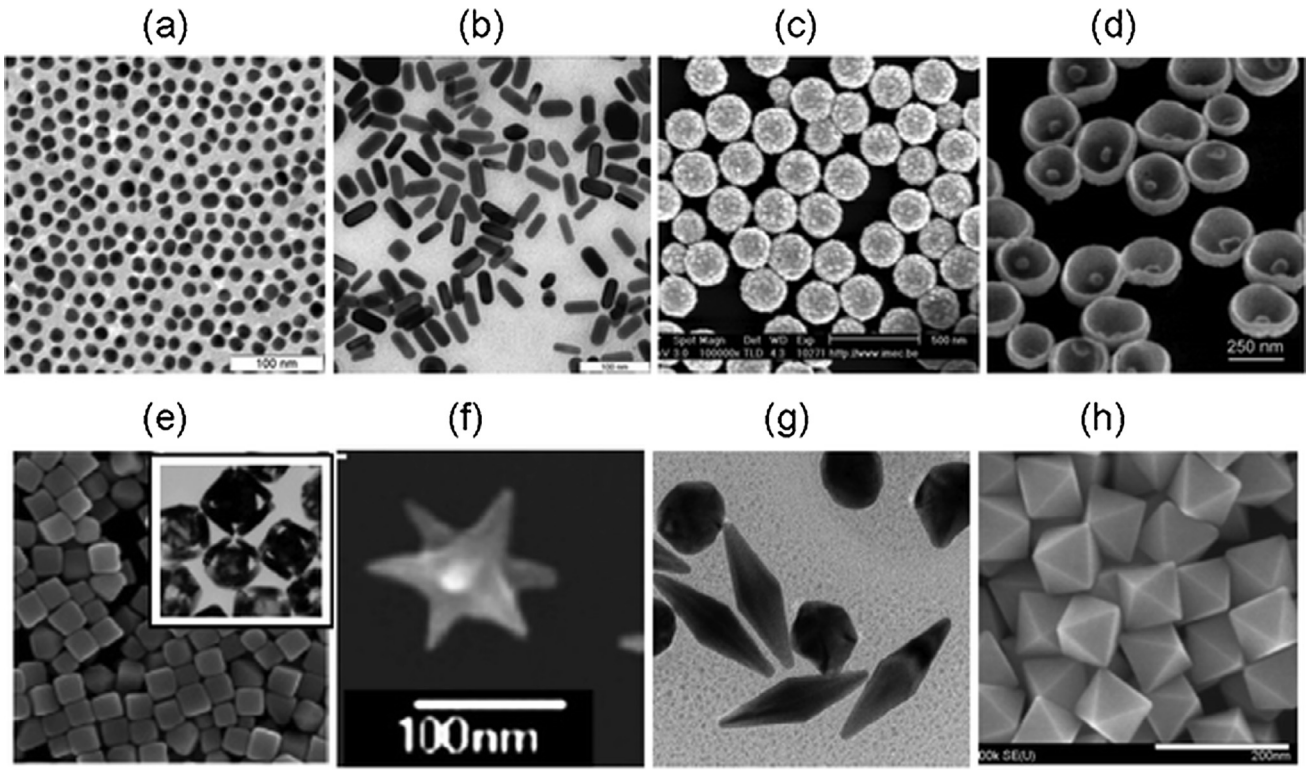

Figure 8 TEM images of different form of gold NPs, synthesized by different techniques (Khlebtsov and Dykman, 2011, 2010a, 2010b).

(Swinehart, 1962). These techniques give information about the absorption, reflectance, luminescence and phosphorescence properties of NPs. It is widely known that NPs especially metallic and semiconductor NPs possess different colors and therefore, best harmonized for photo-related applications. So, it is always interesting to know the value of absorption and reflectance of these materials to understand the basic mechanism for each application. Ultraviolet–visible (UV–Vis), photoluminescence (PL) and the null ellipsometer are the well-known optical instruments, which can be used to study the optical properties of NPs materials.

The UV/vis- diffuse reflectance spectrometer (DRS) is a fully equipped device which can be used to measure the optical absorption, transmittance and reflectance. The former two are supplementary to each other while the latter (DRS) is a special technique use for sold samples mostly. The method is exceptionally acceptable for the determination of bandgaps of NPs and other nanomaterials. Bandgap of materials is very important to conclude about the photoactivity and conductance of the material. The carbon nanodot-carbon nitride (C_3N_4) was found to be a metal free water splitting photocatalyst. The photo ability of this material is directly correlated to the bandgap value of 2.74–2.77 eV, which was calculated using UV–Vis spectroscopy (Liu et al., 2015a, 2015b). Similarly, this technique also use to see the absorption shift in case of doping, composite formation or heterostructure NPs materials. Peng et al. synthesis MMT, $LaFeO_3$ and $LaFeO_3$/MMT nanocomposites and studied variation in their electromagnetic radiations absorption through UV–vis DRS to reconnoiter their optical characteristics. The strong red shift observed in case of nanocomposite as compared to pristine MMT and $LaFeO_3$ NPs. $LaFeO_3$ and $LaFeO_3$/MMT displayed rather broad absorption band from 400 to 620 nm, showing decrease in their bandgap. This property makes these catalysts considerable for solar light driven photocatalysis (Peng et al., 2016).

In addition to UV, PL also considers valuable technique to study the optical properties of the photoactive NPs and other nanomaterials. This technique offers additional information about the absorption or emission capacity of the materials and their effect on the overall excitation time of photoexcitons. Thus, it provides significant information about the charge recombination and half-life of the excited materials in their conductance band, which are useful for all photo related and imaging applications. The PL spectrum can be recorded as emission or absorbance depending on the nature of study. Fig. 11 shows a typical PL spectrum of pristine and modified ZnO NPs. It is evident from this figure that pristine ZnO NPs show high PL intensity as compared to CdS modified ZnO NPs. The gold embedded CdS/Au/ZnO composite shows the lowest intensity. This quenching from pure ZnO to CdS/Au/ZnO can be attributed to the decrease in the rate of charge recombination and larger lifetime of photoexcitons in the latter case (Yu et al., 2013). In addition, this technique is successfully used to determine the thickness of layer (Lin et al., 2015), doping quantity of (Gupta et al., 2013; Pal et al., 2012) material and defects/oxygen vacancies determination (Torchynska et al., 2016) of NPs.

Similarly, Wan et al. determined the values of refractive index and extinction coefficient for hollow gold NPs (HG-NPs) via spectroscopic ellipsometry. They prepared a series of HG-NPs, with different morphologies and plasmonic properties and the optical constants were calculated. The values were compared with the optical constant values of solid gold NPs, which gave good indication to use these materials in

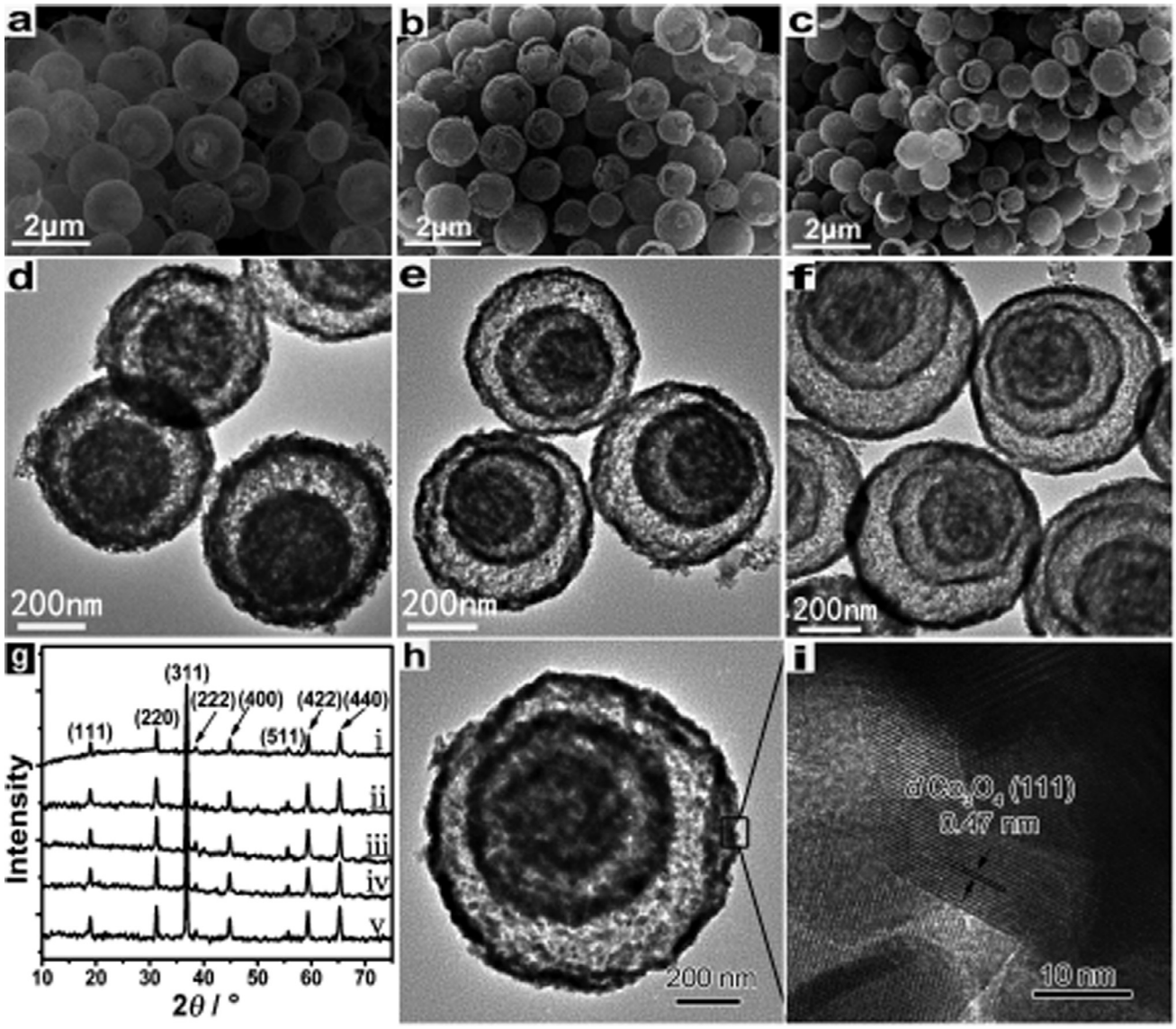

Figure 9 SEM (a–c, h), TEM (d–f), XRD patterns (g) and HRTEM (i) images of double, triple and quadruple Co_3O_4 hollow shells (Wang et al., 2013).

chemical sensing applications due to their sensitive nature as revealed from ellipsometric values (Wan et al., 2009).

5. Physicochemical properties of NPs

As discussed earlier, various physicochemical properties such as large surface area, mechanically strong, optically active and chemically reactive make NPs unique and suitable applicants for various applications. Some of their important properties are discuss in the following section.

5.1. Electronic and optical properties

The optical and electronic properties of NPs are interdependent to greater extent. For instance, noble metals NPs have size dependent optical properties and exhibit a strong UV–visible extinction band that is not present in the spectrum of the bulk metal. This excitation band results when the incident photon frequency is constant with the collective excitation of the conduction electrons and is known as the localized surface plasma resonance (LSPR). LSPR excitation results in the wavelength selection absorption with extremely large molar excitation coefficient resonance Ray light scattering with efficiency equivalent to that of ten fluorophores and enhanced local electromagnetic fields near the surface of NPs that enhanced spectroscopies. It is well established that the peak wavelength of the LSPR spectrum is dependent upon the size, shape and interparticle spacing of the NPs as well as its own dielectric properties and those of its local environment including the substrate, solvents and adsorbates (Eustis and El-Sayed, 2006). Gold colloidal NPs are accountable for the rusty colors seen in blemished glass door/windows, while Ag NPs are typically yellow. Actually, the free electrons on the surface in these NPs (d electrons in Ag and gold) are freely transportable through the nanomaterial. The mean free path for

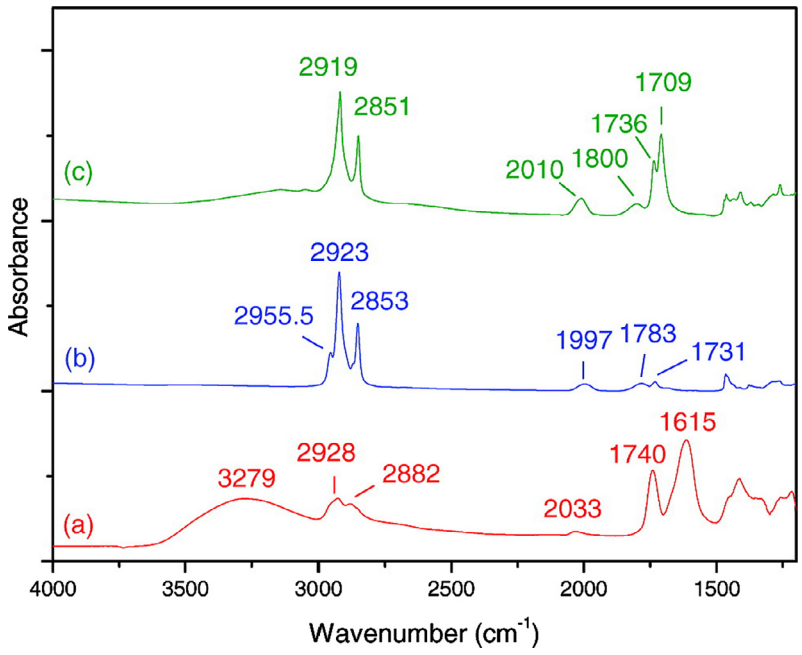

Figure 10 FTIR spectra of platinum (1.7 nm) (a) extracted from polyol, (b) dodecanethiol coated Pt, and (c) MUDA coated Pt (Dablemont et al., 2008).

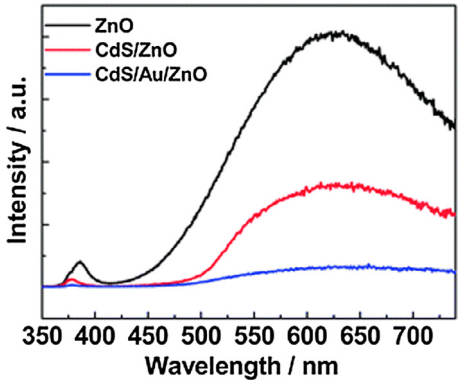

Figure 11 Photoluminescence (PL) spectra of pristine ZnO, CdS/ZnO, and CdS/Au/ZnO measured with 270 nm excitation wavelength at normal temperature (Yu et al., 2013).

Ag and gold is ~50 nm, which is more than the NPs size of these materials. Thus, no scattering is expected from the bulk, upon light interaction, instead they set into a standing resonance conditions, which is responsible for LSPR in these NPs (Fig. 12) (Khlebtsov and Dykman, 2010a, 2010b).

5.2. Magnetic properties

Magnetic NPs are of great curiosity for investigators from an eclectic range of disciplines, which include heterogenous and homogenous catalysis, biomedicine, magnetic fluids, data storage magnetic resonance imaging (MRI), and environmental remediation such as water decontamination. The literature revealed that NPs perform best when the size is < critical value i.e. 10–20 nm (Reiss and Hütten, 2005). At such low scale the magnetic properties of NPs dominated effectively, which make these particle priceless and can be used in different applications (Faivre and Bennet, 2016; Priyadarshana et al., 2015; Reiss and Hütten, 2005; Zhu et al., 1994). The uneven electronic distribution in NPs leads to magnetic property. These properties are also dependent on the synthetic protocol and various synthetic methods such as solvothermal (Qi et al., 2016), co-precipitation, micro-emulsion, thermal decomposition, and flame spray synthesis can be used for their preparation (Wu et al., 2008).

5.3. Mechanical properties

The distinct mechanical properties of NPs allow researchers to look for novel applications in many important fields such as tribology, surface engineering, nanofabrication and nanomanufacturing. Different mechanical parameters such as elastic modulus, hardness, stress and strain, adhesion and friction can be surveyed to know the exact mechanical nature of NPs. Beside these parameters surface coating, coagulation, and lubrication also aid to mechanical properties of NPs (Guo et al., 2014) (see Scheme 4). NPs show dissimilar mechanical properties as compared to microparticles and their bulk materials. Moreover, in a lubricated or greased contact, the contrast in the stiffness between NPs and the contacting external surface controls whether the NPs are indented into the plan surface or deformed when the pressure at contact is significantly large. This important information could divulge how the NPs perform in the contact situation. Decent controls over mechanical features of NPs and their interactions with any kind of surface are vital for enlightening the surface quality and elevating material removal. Fruitful outcomes in these fields generally need a deep insight into the basics of the mechanical properties of NPs, such as elastic modulus and hardness, movement law, friction and interfacial adhesion and their size dependent characteristics (Guo et al., 2014).

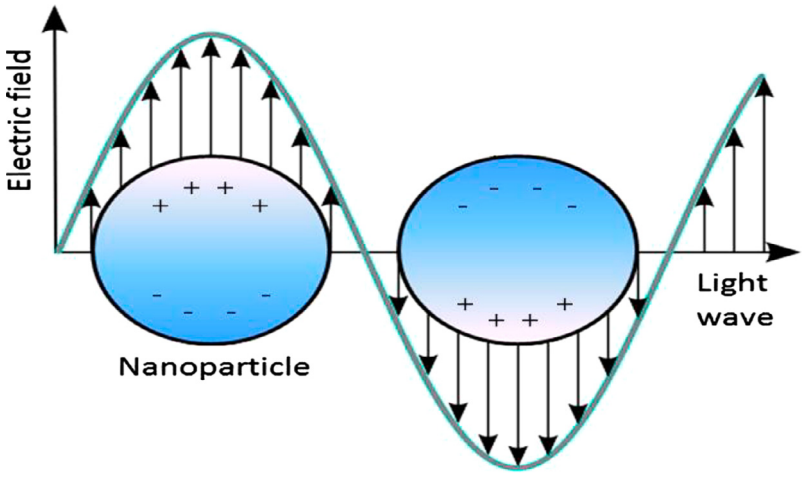

Figure 12 Graphical illustration exemplifying the localized surface plasmon (LSPR) on nanoparticle outer surface (Khlebtsov and Dykman, 2010a, 2010b).

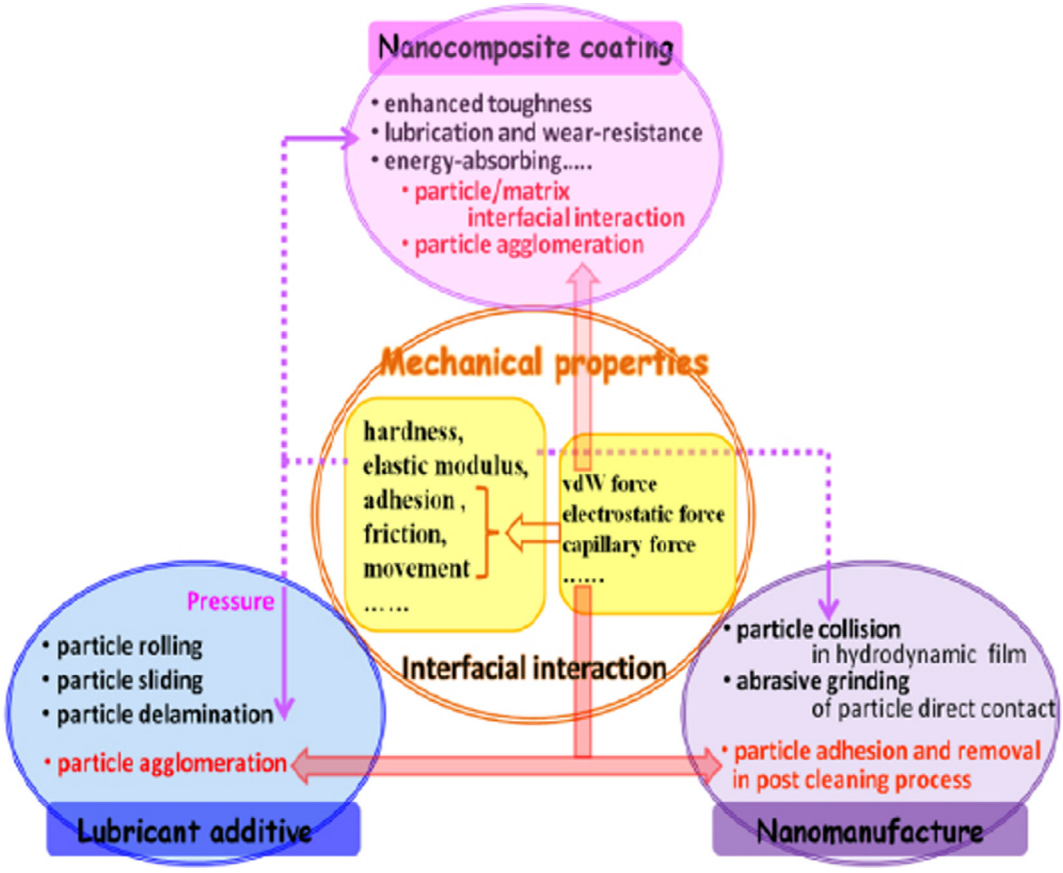

Scheme 4 Schematic view of the mechanical properties and their applications (Guo et al., 2014).

5.4. Thermal properties

It is well-known fact that metals NPs have thermal conductivities higher than those of fluids in solid form. For example, the thermal conductivity of copper at room temperature is about 700 times greater than that of water and about 3000 times greater than that of engine oil. Even oxides such as alumina (Al_2O_3) have thermal conductivity higher than that of water. Therefore, the fluids containing suspended solid particles are expected to display significantly enhanced thermal conductivities relative to those of conventional heat transfer fluids. Nanofluids are produced by dispersing the nanometric scales solid particles into liquid such as water, ethylene glycol or oils. Nanofluids are expected to exhibit superior properties relative

to those of conventional heat transfer fluids and fluids containing microscopic sized particles. Because the heat transfer takes place at the surface of the particles, it is desirable to use the particles with large total surface area. The large total surface area also increases the stability suspension (Lee et al., 1999). Recently it has been demonstrated that the nanofluids consisting of CuO or Al_2O_3 NPs in water or ethylene exhibit advance thermal conductivity (Cao, 2002).

6. Applications of NPs

Considering the unique properties discussed in Section 5, NPs can be used in variety of applications. Some important of these are given below.

6.1. Applications in drugs and medications

Nano-sized inorganic particles of either simple or complex nature, display unique, physical and chemical properties and represent an increasingly important material in the development of novel nanodevices which can be used in numerous physical, biological, biomedical and pharmaceutical applications (Loureiro et al., 2016; Martis et al., 2012; Nikalje, 2015).

NPs have drawn increasing interest from every branch of medicine for their ability to deliver drugs in the optimum dosage range often resulting in increased therapeutic efficiency of the drugs, weakened side effects and improved patient compliance (Alexis et al., 2008). Iron oxide particles such as magnetite (Fe_3O_4) or its oxidized form maghemite (Fe_2O_3) are the most commonly employed for biomedical applications (Ali et al., 2016). The selection of NPs for achieving efficient contrast for biological and cell imaging applications as well as for photo thermal therapeutic applications is based on the optical properties of NPs. Mie theory and discrete dipole approximation method can be used to calculate absorption and scattering efficiencies and optical resonance wavelength for the commonly used classes of NPs i.e. Au NPs, silica-Au NPs and Au nanorods (Jain et al., 2006). The development of hydrophilic NPs as drug carrier has represented over the last few years an important challenge. Among the different approaches, polyethylene oxide (PEO) and polylactic acid (PLA) NPs have been revealed as very promising system for the intravenous administration of drugs (Calvo et al., 1997). Superparamagnetic iron oxide NPs with appropriate surface chemistry can be used for numerous in vivo applications such as MRI contrast enhancement, tissue repair, and immunoassay, detoxification of biological fluids hyperthermia, drugs delivery and cell separation. All of these biomedical applications require that the NPs have high magnetization value, a size smaller than 100 nm and a narrow particle size distribution (Laurent et al., 2010). The detection of analytes in tissue sections can be accomplished through antigen-antibody interactions using antibodies labeled with fluorescent dyes, enzymes, radioactive compounds or colloidal Au (Khlebtsov and Dykman, 2010b).

Over past few decades these has been considerable interest in developing biodegradable NPs as effective drug delivery devices (Zhang and Saltzman, 2013). Various polymers have been used in drug delivery research as they can effectively deliver the drugs to the target site thus increases the therapeutic benefit, while minimizing side effects. The controlled release of pharmacologically active drugs to the precise action site at the therapeutically optimum degree and dose regimen has been a major goal in designing such devices.

Liposomes have been used as a potential drug carrier instead of conventional dosage forms because of their unique advantages which include ability to protect drugs from degradation, target to the site of action and reduce the noxiousness and other side effects. However developmental work on liposome drugs has been restricted due to inherent health issues such as squat encapsulation efficiency, rapid water leakage in the commodity of blood components and very poor storage, and stability. On the other hand, polymeric NPs promise some critical advantages over these materials i.e. liposomes. For instance, NPs help to increase the ratability of drugs or problems and possess convenient controlled drug release properties.

Most of the semiconductor and metallic NPs have immense potential for cancer diagnosis and therapy on account of their surface plasmon resonance (SPR) enhanced light scattering and absorption. Au NPs efficiently convert the strong absorbed light into localized heat which can be exploited for the selective laser photo thermal therapy of cancer (Prashant et al., 2007). Beside this the antineoplastic effect of NPs is also effectively employed to inhibit the tumor growth. The multihydroxylated $[Gd@C_{82}(OH)_{22}]_n$ NPs showed antineoplastic activity with good efficiency and lower toxicity (Chen et al., 2005). Ag NPs are being used increasingly in wound dressings, catheters and various households' products due to their antimicrobial activity (AshaRani et al., 2009). Antimicrobial agents are extremely vital in textile, medicine, water disinfection and food packaging. Therefore, the antimicrobial characteristics of inorganic NPs add more potency to this important aspect, as compared to organic compounds, which are relatively toxic to the biological systems (Hajipour et al., 2012). These NPs are functionalized with various groups to overcome the microbial species selectively. TiO_2, ZnO, $BiVO_4$, Cu- and Ni-based NPs have been utilized for this purpose due to their suitable antibacterial efficacies (Akhavan et al., 2011; Pant et al., 2013; Qu et al., 2016; Yin et al., 2016).

6.2. Applications in manufacturing and materials

Nanocrystalline materials provide very interesting substances for material science since their properties deviate from respective bulk material in a size dependent manner. Manufacture NPs display physicochemical characteristics that induce unique electrical, mechanical, optical and imaging properties that are extremely looked-for in certain applications within the medical, commercial, and ecological sectors (Dong et al., 2014; Ma, 2003; Todescato et al., 2016). NPs focus on the characterization, designing and engineering of biological as well as non-biological structures < than 100 nm, which show unique and novel functional properties. The potential benefits of nanotechnology have been documented by many manufacturer at high and low level and marketable products are already being mass-produced such as microelectronics, aerospace and pharmaceutical industries (Weiss et al., 2006). Among the nanotechnology consumer products to date, health fitness products from the largest category, followed by the electronic and computer category as well as home and garden category. Nanotechnology has been touted as the next revolution in many industries including food processing and packing.

Resonant energy transfer (RET) system consisting of organic dye molecules and noble metals NPs have recently gamed considerable interest in bio photonics as well as in material science (Lei et al., 2015). The presence of NPs in commercially available products is becoming more common.

Metals NPs such as noble metals, including Au and Ag have many colors in the visible region based on plasmon resonance, which is due to collective oscillations of the electrons at the surface of NPs (Khlebtsov and Dykman, 2010a, 2010b; Unser et al., 2015). The resonance wavelength strong depends on size and shape of NPs, the interparticle distance, and the dielectric property of the surrounding medium. The unique plasmon absorbance features of these noble metals NPs have been exploited for a wide variety of applications including chemical sensors and biosensors (Unser et al., 2015).

6.3. Applications in the environment

The increasing area of engineered NPs in industrial and household applications leads to the release of such materials into the environment. Assessing the risk of these NPs in the environment requires on understanding of their mobility, reactivity, Eco toxicity and persistency (Ripp and Henry, 2011; Zhuang and Gentry, 2011). The engineering material applications can increase the concentration of NPs in groundwater and soil which presents the most significant exposure avenues for assessing environmental risks (Golobič et al., 2012; Masciangioli and Zhang, 2003). Due to high surface to mass ratio natural NPs play an important role in the solid/water partitioning of contaminants can be absorbed to the surface of NPs, co-precipitated during the formation of natural NPs or trapped by aggregation of NPs which had contaminants adsorbed to their surface. The interaction of contaminants with NPs is dependent on the NPs characteristics, such as size, composition, morphology, porosity, aggregation/disaggregation and aggregate structure. The luminophores are not safe in the environment and are protected from the environmental oxygen when they are doped inside the silica network (Swadeshmukul et al., 2001).

Most of environmental applications of nanotechnology fall into three categories:

1. Environmentally benign sustainable products (e.g. green chemistry or pollution prevention).
2. Remediation of materials contaminated with hazardous substances and
3. Sensors for environmental stages (Tratnyek and Johnson, 2006).

The removal of heavy metals such as mercury, lead, thallium, cadmium and arsenic from natural water has attracted considerable attention because of their adverse effects on environmental and human health. Superparamagnetic iron oxide NPs are an effective sorbent material for this toxic soft material. So, for no measurements of engineered NPs in the environment have been available due to the absence of analytical methods, able to quantify trace concentration of NPs (Mueller and Nowack, 2008). Photodegradation by NPs is also very common practice and many nanomaterials are utilized for this purpose. Rogozea et al. used NiO/ZnO NPs modified silica in the tandem fashion for photodegradation purpose. The high surface area of NPs due to very small size (<10 nm), facilitated the efficient photodegradation reaction (Rogozea et al., 2017). The same group has reported the synthesis of variety of NPs and reported their optical, florescence and degradation applications (Olteanu et al., 2016a, 2016b; Rogozea et al., 2016).

6.4. Applications in electronics

There has been growing interest in the development of printed electronics in last few years because printed electronics offer attractive to traditional silicon techniques and the potential for low cost, large area electronics for flexible displays, sensors. Printed electronics with various functional inks containing NPs such as metallic NPs, organic electronic molecules, CNTs and ceramics NPs have been expected to flow rapidly as a mass production process for new types of electronic equipment (Kosmala et al., 2011).

Unique structural, optical and electrical properties of one dimensional semiconductor and metals make them the key structural block for a new generation of electronic, sensors and photonic materials (Holzinger et al., 2014; Millstone et al., 2010; Shaalan et al., 2016).

The good example of the synergism between scientific discovery and technological development is the electronic industry, where discoveries of new semiconducting materials resulted in the revolution from vacuumed tubes to diodes and transistors, and eventually to miniature chips (Cushing et al., 2004).

The important characteristics of NPs are facile manipulation and reversible assembly which allow for the possibility of incorporation of NPs in electric, electronic or optical devices such as "bottom up" or "self-assembly" approaches are the bench mark of nanotechnology (O'Brien et al., 2001).

6.5. Applications in energy harvesting

Recent studies warned us about the limitations and scarcity of fossil fuels in coming years due to their nonrenewable nature. Therefore, scientists shifting their research strategies to generate renewable energies from easily available resources at cheap cost. They found that NPs are the best candidate for this purpose due to their, large surface area, optical behavior and catalytic nature. Especially in photocatalytic applications, NPs are widely used to generate energy from photoelectrochemical (PEC) and electrochemical water splitting (Avasare et al., 2015; Mueller and Nowack, 2008; Ning et al., 2016). Beside water splitting, electrochemical CO_2 reduction to fuels precursors, solar cells and piezoelectric generators also offered advance options to generate energy (Fang et al., 2013; Gawande et al., 2016; Lei et al., 2015; Li et al., 2016; Nagarajan et al., 2014; Sagadevan, 2015; Young et al., 2012; Zhou et al., 2016). NPs also use in energy storage applications to reserve the energy into different forms at nanoscale level (Greeley and Markovic, 2012; Liu et al., 2015a, 2015b; Sagadevan, 2015; Wang and Su, 2014). Recently, nanogenerators are created, which can convert the mechanical energy into electricity using piezoelectric, which is an unconventional approach to generate energy (Wang et al., 2015). Fig. 13 shows some energy generating devices, and uses NPs.

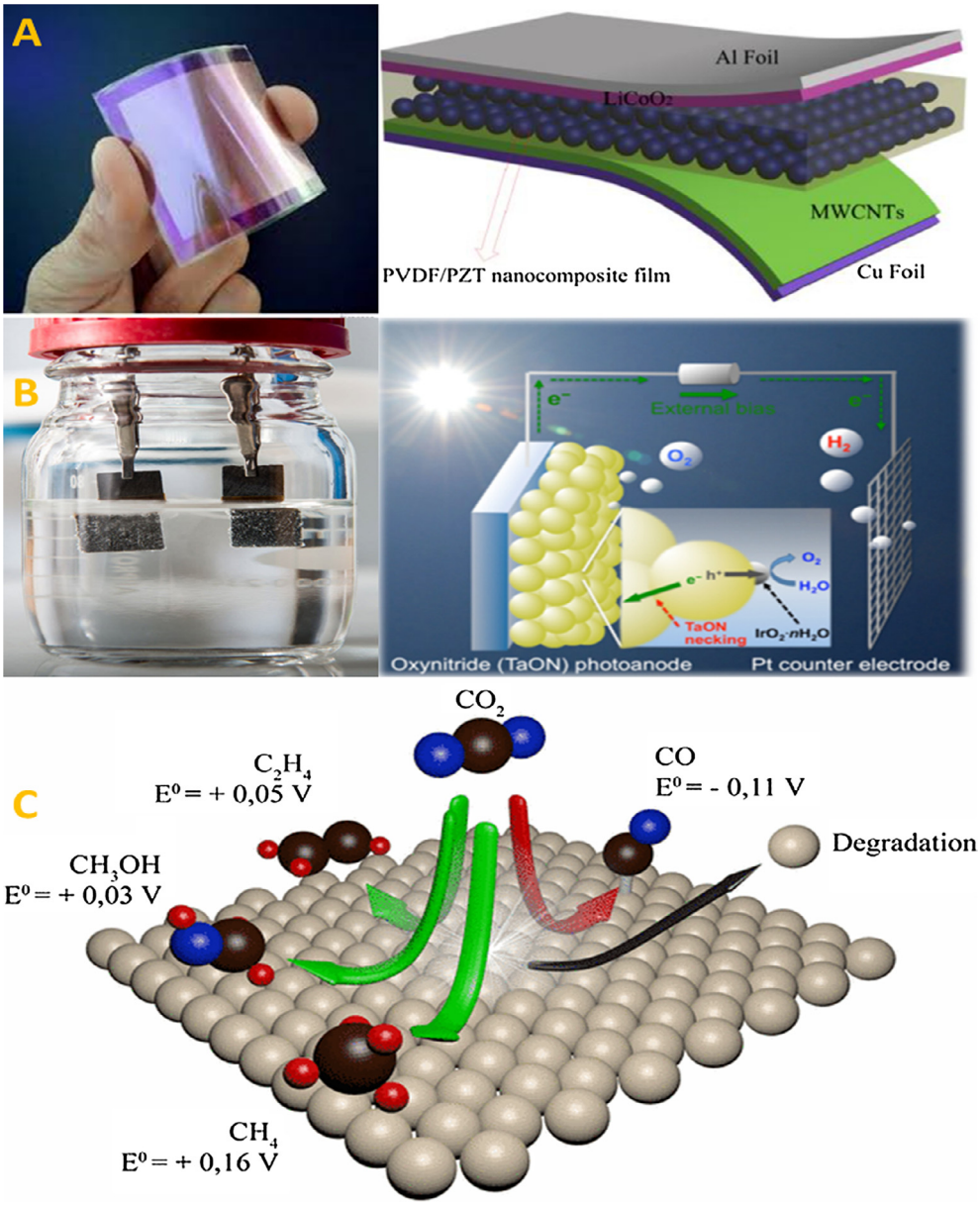

Figure 13 Energy generation approaches from (A) Piezoelectrics actuators (B) Water splitting (C) CO_2 reduction.

6.6. Applications in mechanical industries

As revealed from their mechanical properties through excellent young modulus, stress and strain properties, NPs can offer many applications in mechanical industries especially in coating, lubricants and adhesive applications. Besides, this property can be useful to achieve mechanically stronger nanodevices for various purposes. Tribological properties can be controlled at nanoscale level by embedding NPs in the metal and polymer matrix to increase their mechanical strengths. It is because, the rolling mode of NPs in the lubricated contact area could provide very low friction and wear. In addition, NPs offer good sliding and delamination properties, which could also effect in low friction and wear, and hence increase lubrication effect (Guo et al., 2014). Coating can lead to various mechanically strong characteristics, as it improves toughness and wear resistance. Alumina, Titania and carbon based NPs successfully demonstrated to get the desirable mechanical properties in coatings (Kot et al., 2016; Mallakpour and Sirous, 2015; Shao et al., 2012).

7. Toxicity of NP

Beside many industrial and medical applications, there are certain toxicities which are associated with NPs and other nanomaterials (Bahadar et al., 2016; Ibrahim, 2013; Khlebtsov and Dykman, 2011, 2010b) and basic knowledge is required for these toxic effects to encounter them properly. NPs surreptitiously enter the environment through water, soil, and air during various human activities. However, the application of NPs

for environmental treatment deliberately injects or dumps engineered NPs into the soil or aquatic systems. This has resultantly attracted increasing concern from all stakeholders. The advantages of magnetic NPs such as their small size, high reactivity and great capacity, could become potential lethal factors by inducing adverse cellular toxic and harmful effects, unusual in micron-sized counter parts. Studies also illustrated that NPs can enter organisms during ingestion or inhalation and can translocate within the body to various organs and tissues where the NPs have the possibility to exert the reactivity being toxicology effects. Although some studies have also addressed the toxicological effects of NPs on animal cells and plant cells the toxicological studies with magnetic NPs on plants to date are still limited. The uses of Ag NPs in numerous consumer products lead them to their release to the aquatic environment and become a source of dissolved Ag and thus exert toxic effects on aquatic organisms including bacteria, algae, fish and daphnia (Navarro et al., 2008). The respiratory system represents an unique target for the potential toxicity of NPs due to the fact that in addition to being the portal of entry for inhaled particles, it also receives the entire cardiac output (Ferreira et al., 2013). NPs are used in bio applications widely but despite the rapid progress and early acceptance of nanobiotechnology the potential for adverse health effects due to prolong exposure at various concentrations levels in human in the environment has not yet been established. However, the environmental impact of NPs is expected to increase in the future. One of the NPs toxicity is the ability to organize around the protein concentration that depends on particles size, curvature, shape and surface characteristics charge, functionalized groups, and free energy. Due to this binding, some particles generate adverse biological outcomes through protein unfolding, fibrillation, thiol crosslinking, and loss of enzymatic activity. Another paradigm is the release of toxic ions when the thermodynamic properties of materials favor particles dissolution in a suspending medium or biological environment (Xia et al., 2008).

NPs tend to aggregate in hard water and seawater and are greatly influenced by the specific type of organic matter or other natural particles (colloids) present in fresh water. The state of dispersion will alter the ecotoxicity, but many abiotic factors that influence this, such as pH, salinity, and the presence of organic matters remain to be systematically investigated as part of ecotoxicological studies (Handy et al., 2008).

8. Conclusion

In this review, we presented a detail overview about NPs, their types, synthesis, characterizations, physiochemical properties and applications. Through different characterization techniques such as SEM, TEM and XRD, it was revealed that NPs have size ranges from few nanometer to 500 nm. While the morphology is also controllable. Due to their tiny size, NPs have large surface area, which make them suitable candidate for various applications. Beside this, the optical properties are also dominant at that size, which further increase the importance of these materials in photocatalytic applications. Synthetic techniques can be useful to control the specific morphology, size and magnetic properties of NPs. Though NPs are useful for many applications, but still there are some health hazard concerns due to their uncontrollable use and discharge to natural environment, which should be consider for make the use of NPs more convenient and environmental friendly.

9. Recommendations

Our recommendation for future work is that different reaction parameters such as temperature, pressure, time, and pH. can play important role in controlling the shape and morphology of the NPs materials, so that should be optimize for achieving specific characteristic product. Beside this for good implications and properties study specific characterization techniques should be used. More importantly environmental issued should be taken into account before using these materials for any applications, especially in case of heavy metals, which are prone to environmental hazards and can also affect the livings as well.

References

Abd Ellah, N.H., Abouelmagd, S.A., 2016. Surface functionalization of polymeric nanoparticles for tumor drug delivery: approaches and challenges. Expert Opin. Drug Deliv. 1–14. http://dx.doi.org/10.1080/17425247.2016.1213238.

Abouelmagd, S.A., Meng, F., Kim, B.-K., Hyun, H., Yeo, Y., 2016. Tannic acid-mediated surface functionalization of polymeric nanoparticles. ACS Biomater. Sci. Eng., 6b00497 http://dx.doi.org/10.1021/acsbiomaterials.6b004.

Ahmed, S., Annu, S., Yudha, S.S., 2016. Biosynthesis of gold nanoparticles: a green approach. J. Photochem. Photobiol. B: Biol. 161, 141–153. http://dx.doi.org/10.1016/j.jphotobiol.2016.04.034.

Akhavan, O., Azimirad, R., Safa, S., Hasani, E., 2011. CuO/$Cu(OH)_2$ hierarchical nanostructures as bactericidal photocatalysts. J. Mater. Chem. 21, 9634. http://dx.doi.org/10.1039/c0jm04364h.

Alexis, F., Pridgen, E., Molnar, L.K., Farokhzad, O.C., 2008. Factors affecting the clearance and biodistribution of polymeric nanoparticles. Mol. Pharm. 5, 505–515. http://dx.doi.org/10.1021/mp800051m.

Ali, A., Zafar, H., Zia, M., Ul Haq, I., Phull, A.R., Ali, J.S., Hussain, A., 2016. Synthesis, characterization, applications, and challenges of iron oxide nanoparticles. Nanotechnol. Sci. Appl. 9, 49–67. http://dx.doi.org/10.2147/NSA.S99986.

Ali, S., Khan, I., Khan, S.A., Sohail, M., Ahmed, R., Rehman, A., Ur Ansari, M.S., Morsy, M.A., 2017. Electrocatalytic performance of Ni@Pt core–shell nanoparticles supported on carbon nanotubes for methanol oxidation reaction. J. Electroanal. Chem. 795, 17–25. http://dx.doi.org/10.1016/j.jelechem.2017.04.040.

Aqel, A., El-Nour, K.M.M.A., Ammar, R.A.A., Al-Warthan, A., 2012. Carbon nanotubes, science and technology part (I) structure, synthesis and characterisation. Arab. J. Chem. 5, 1–23. http://dx.doi.org/10.1016/j.arabjc.2010.08.022.

AshaRani, P.V., Low Kah Mun, G., Hande, M.P., Valiyaveettil, S., 2009. Cytotoxicity and genotoxicity of silver nanoparticles in human cells. ACS Nano 3, 279–290. http://dx.doi.org/10.1021/nn800596w.

Astefanei, A., Núñez, O., Galceran, M.T., 2015. Characterisation and determination of fullerenes: a critical review. Anal. Chim. Acta 882, 1–21. http://dx.doi.org/10.1016/j.aca.2015.03.025.

Avasare, V., Zhang, Z., Avasare, D., Khan, I., Qurashi, A., 2015. Room-temperature synthesis of TiO_2 nanospheres and their solar driven photoelectrochemical hydrogen production. Int. J. Energy Res. 39, 1714–1719. http://dx.doi.org/10.1002/er.3372.

Bahadar, H., Maqbool, F., Niaz, K., Abdollahi, M., 2016. Toxicity of nanoparticles and an overview of current experimental models. Iran. Biomed. J. 20, 1–11. http://dx.doi.org/10.7508/ibj.2016.01.001.

Barrak, H., Saied, T., Chevallier, P., Laroche, G., M'nif, A., Hamzaoui, A.H., 2016. Synthesis, characterization, and functionalization of ZnO nanoparticles by N-(trimethoxysilylpropyl)

ethylenediamine triacetic acid (TMSEDTA): investigation of the interactions between phloroglucinol and ZnO@TMSEDTA. Arab. J. Chem. http://dx.doi.org/10.1016/j.arabjc.2016.04.019.

Bello, S.A., Agunsoye, J.O., Hassan, S.B., 2015. Synthesis of coconut shell nanoparticles via a top down approach: assessment of milling duration on the particle sizes and morphologies of coconut shell nanoparticles. Mater. Lett. http://dx.doi.org/10.1016/j.matlet.2015.07.063.

Biswas, A., Bayer, I.S., Biris, A.S., Wang, T., Dervishi, E., Faupel, F., 2012. Advances in top–down and bottom–up surface nanofabrication: techniques, applications & future prospects. Adv. Coll. Interface. Sci. 170, 2–27. http://dx.doi.org/10.1016/j.cis.2011.11.001.

Calvo, P., Remuoon-Lopez, C., Vila-Jato, J.L., Alonso, M.J., 1997. Novel hydrophilic chitosan-polyethylene oxide nanoparticles as protein carriers. J. Appl. Polym. Sci. 63, 125–132. http://dx.doi.org/10.1002/(SICI)1097-4628(19970103)63:1*125::AID-APP13*3.0.CO;2-4.

Cao, Y.C., 2002. Nanoparticles with Raman spectroscopic fingerprints for DNA and RNA detection. Science 80 (297), 1536–1540. http://dx.doi.org/10.1126/science.297.5586.1536.

Chen, C., Xing, G., Wang, J., Zhao, Y., Li, B., Tang, J., Jia, G., Wang, T., Sun, J., Xing, L., Yuan, H., Gao, Y., Meng, H., Chen, Z., Zhao, F., Chai, Z., Fang, X., 2005. Multihydroxylated [Gd@C 82 (OH) 22] n nanoparticles: antineoplastic activity of high efficiency and low toxicity. Nano Lett. 5, 2050–2057. http://dx.doi.org/10.1021/nl051624b.

Cushing, B.L., Kolesnichenko, V.L., O'Connor, C.J., 2004. Recent advances in the liquid-phase syntheses of inorganic nanoparticles. Chem. Rev. 104, 3893–3946. http://dx.doi.org/10.1021/cr030027b.

Dablemont, C., Lang, P., Mangeney, C., Piquemal, J.-Y., Petkov, V., Herbst, F., Viau, G., 2008. FTIR and XPS study of Pt nanoparticle functionalization and interaction with alumina. Langmuir 24, 5832–5841. http://dx.doi.org/10.1021/la7028643.

Dong, H., Wen, B., Melnik, R., 2014. Relative importance of grain boundaries and size effects in thermal conductivity of nanocrystalline materials. Sci. Rep. 4, 7037. http://dx.doi.org/10.1038/srep07037.

Dreaden, E.C., Alkilany, A.M., Huang, X., Murphy, C.J., El-Sayed, M.A., 2012. The golden age: gold nanoparticles for biomedicine. Chem. Soc. Rev. 41, 2740–2779. http://dx.doi.org/10.1039/C1CS15237H.

Elliott, J.A., Shibuta, Y., Amara, H., Bichara, C., Neyts, E.C., 2013. Atomistic modelling of CVD synthesis of carbon nanotubes and graphene. Nanoscale 5, 6662. http://dx.doi.org/10.1039/c3nr01925j.

Emery, A.A., Saal, J.E., Kirklin, S., Hegde, V.I., Wolverton, C., 2016. High-throughput computational screening of perovskites for thermochemical water splitting applications. Chem. Mater. 28. http://dx.doi.org/10.1021/acs.chemmater.6b01182.

Eustis, S., El-Sayed, M.A., 2006. Why gold nanoparticles are more precious than pretty gold: noble metal surface plasmon resonance and its enhancement of the radiative and nonradiative properties of nanocrystals of different shapes. Chem. Soc. Rev. 35, 209–217. http://dx.doi.org/10.1039/B514191E.

Fagerlund, G., 1973. Determination of specific surface by the BET method. Matériaux Constr. 6, 239–245. http://dx.doi.org/10.1007/BF02479039.

Faivre, D., Bennet, M., 2016. Materials science: magnetic nanoparticles line up. Nature 535, 235–236. http://dx.doi.org/10.1038/535235a.

Fang, X.-Q., Liu, J.-X., Gupta, V., 2013. Fundamental formulations and recent achievements in piezoelectric nano-structures: a review. Nanoscale 5, 1716. http://dx.doi.org/10.1039/c2nr33531j.

Ferreira, A.J., Cemlyn-Jones, J., Robalo Cordeiro, C., 2013. Nanoparticles, nanotechnology and pulmonary nanotoxicology. Rev. Port. Pneumol. 19, 28–37. http://dx.doi.org/10.1016/j.rppneu.2012.09.003.

Filipe, V., Hawe, A., Jiskoot, W., 2010. Critical evaluation of nanoparticle tracking analysis (NTA) by nanosight for the measurement of nanoparticles and protein aggregates. Pharm. Res. 27, 796–810. http://dx.doi.org/10.1007/s11095-010-0073-2.

Ganesh, M., Hemalatha, P., Peng, M.M., Jang, H.T., 2017. One pot synthesized Li, Zr doped porous silica nanoparticle for low temperature CO_2 adsorption. Arab. J. Chem. 10, S1501–S1505.

Garrigue, P., Delville, M.-H., Labrugère, C., Cloutet, E., Kulesza, P. J., Morand, J.P., Kuhn, A., 2004. Top–down approach for the preparation of colloidal carbon nanoparticles. Chem. Mater. 16, 2984–2986. http://dx.doi.org/10.1021/cm049685i.

Gawande, M.B., Goswami, A., Felpin, F.-X., Asefa, T., Huang, X., Silva, R., Zou, X., Zboril, R., Varma, R.S., 2016. Cu and Cu-based nanoparticles: synthesis and applications in catalysis. Chem. Rev. 116, 3722–3811. http://dx.doi.org/10.1021/acs.chemrev.5b00482.

Golobič, M., Jemec, A., Drobne, D., Romih, T., Kasemets, K., Kahru, A., 2012. Upon exposure to Cu nanoparticles, accumulation of copper in the isopod *Porcellio scaber* is due to the dissolved cu ions inside the digestive tract. Environ. Sci. Technol. 46, 12112–12119. http://dx.doi.org/10.1021/es3022182.

Greeley, J., Markovic, N.M., 2012. The road from animal electricity to green energy: combining experiment and theory in electrocatalysis. Energy Environ. Sci. 5. http://dx.doi.org/10.1039/c2ee21754f.

Gross, J., Sayle, S., Karow, A.R., Bakowsky, U., Garidel, P., 2016. Nanoparticle tracking analysis of particle size and concentration detection in suspensions of polymer and protein samples: Influence of experimental and data evaluation parameters. Eur. J. Pharm. Biopharm. 104, 30–41. http://dx.doi.org/10.1016/j.ejpb.2016.04.013.

Gujrati, M., Malamas, A., Shin, T., Jin, E., Sun, Y., Lu, Z.-R., 2014. Multifunctional cationic lipid-based nanoparticles facilitate endosomal escape and reduction-triggered cytosolic siRNA release. Mol. Pharm. 11, 2734–2744. http://dx.doi.org/10.1021/mp400787s.

Guo, D., Xie, G., Luo, J., 2014. Mechanical properties of nanoparticles: basics and applications. J. Phys. D Appl. Phys. 47, 13001. http://dx.doi.org/10.1088/0022-3727/47/1/013001.

Gupta, K., Singh, R.P., Pandey, A., Pandey, A., 2013. Photocatalytic antibacterial performance of TiO_2 and Ag-doped TiO_2 against *S. aureus*. *P. aeruginosa* and *E. coli*. Beilstein J. Nanotechnol. 4, 345–351. http://dx.doi.org/10.3762/bjnano.4.40.

Hajipour, M.J., Fromm, K.M., Ashkarran, A. Akbar, de Aberasturi, D. Jimenez, de Larramendi, I.R., Rojo, T., Serpooshan, V., Parak, W.J., Mahmoudi, M., 2012. Antibacterial properties of nanoparticles. Trends Biotechnol. 30, 499–511. http://dx.doi.org/10.1016/j.tibtech.2012.06.004.

Handy, R.D., von der Kammer, F., Lead, J.R., Hassellöv, M., Owen, R., Crane, M., 2008. The ecotoxicology and chemistry of manufactured nanoparticles. Ecotoxicology 17, 287–314. http://dx.doi.org/10.1007/s10646-008-0199-8.

Hisatomi, T., Kubota, J., Domen, K., 2014. Recent advances in semiconductors for photocatalytic and photoelectrochemical water splitting. Chem. Soc. Rev. 43, 7520–7535. http://dx.doi.org/10.1039/C3CS60378D.

Holzinger, M., Le Goff, A., Cosnier, S., 2014. Nanomaterials for biosensing applications: a review. Front. Chem. 2, 63. http://dx.doi.org/10.3389/fchem.2014.00063.

Ibrahim, K.S., 2013. Carbon nanotubes-properties and applications: a review. Carbon Lett. 14, 131–144. http://dx.doi.org/10.5714/CL.2013.14.3.131.

Ingham, B., 2015. X-ray scattering characterisation of nanoparticles. Crystallogr. Rev. 21, 229–303. http://dx.doi.org/10.1080/0889311X.2015.1024114.

Iqbal, N., Khan, I., Yamani, Z.H., Qurashi, A., 2016. Sonochemical assisted solvothermal synthesis of gallium oxynitride nanosheets and their solar-driven photoelectrochemical water-splitting applications. Sci. Rep. 6, 32319. http://dx.doi.org/10.1038/srep32319.

Iravani, S., 2011. Green synthesis of metal nanoparticles using plants. Green Chem. 13, 2638. http://dx.doi.org/10.1039/c1gc15386b.

Jain, P.K., Lee, K.S., El-Sayed, I.H., El-Sayed, M.A., 2006. Calculated absorption and scattering properties of gold nanoparticles of different size, shape, and composition: applications in biological imaging and biomedicine. J. Phys. Chem. B 110, 7238–7248. http://dx.doi.org/10.1021/jp057170o.

Kestens, V., Roebben, G., Herrmann, J., Jämting, Å., Coleman, V., Minelli, C., Clifford, C., De Temmerman, P.-J., Mast, J., Junjie, L., Babick, F., Cölfen, H., Emons, H., 2016. Challenges in the size analysis of a silica nanoparticle mixture as candidate certified reference material. J. Nanopart. Res. 18, 171. http://dx.doi.org/10.1007/s11051-016-3474-2.

Khan, I., Abdalla, A., Qurashi, A., 2017a. Synthesis of hierarchical WO_3 and Bi_2O_3/WO_3 nanocomposite for solar-driven water splitting applications. Int. J. Hydrogen Energy 42, 3431–3439. http://dx.doi.org/10.1016/j.ijhydene.2016.11.105.

Khan, I., Ali, S., Mansha, M., Qurashi, A., 2017b. Sonochemical assisted hydrothermal synthesis of pseudo-flower shaped Bismuth vanadate ($BiVO_4$) and their solar-driven water splitting application. Ultrason. Sonochem. 36, 386–392. http://dx.doi.org/10.1016/j.ultsonch.2016.12.014.

Khan, I., Ibrahim, A.A.M., Sohail, M., Qurashi, A., 2017c. Sonochemical assisted synthesis of RGO/ZnO nanowire arrays for photoelectrochemical water splitting. Ultrason. Sonochem. 37, 669–675. http://dx.doi.org/10.1016/j.ultsonch.2017.02.029.

Khlebtsov, N., Dykman, L., 2011. Biodistribution and toxicity of engineered gold nanoparticles: a review of in vitro and in vivo studies. Chem. Soc. Rev. 40, 1647–1671. http://dx.doi.org/10.1039/C0CS00018C.

Khlebtsov, N., Dykman, L., 2010. Plasmonic nanoparticles. pp. 37–85. http://dx.doi.org/10.1201/9781439806296-c2.

Khlebtsov, N.G., Dykman, L.A., 2010b. Optical properties and biomedical applications of plasmonic nanoparticles. J. Quant. Spectrosc. Radiat. Transf. 111, 1–35. http://dx.doi.org/10.1016/j.jqsrt.2009.07.012.

Kosmala, A., Wright, R., Zhang, Q., Kirby, P., 2011. Synthesis of silver nano particles and fabrication of aqueous Ag inks for inkjet printing. Mater. Chem. Phys. 129, 1075–1080. http://dx.doi.org/10.1016/j.matchemphys.2011.05.064.

Kot, M., Major, Ł., Lackner, J.M., Chronowska-Przywara, K., Janusz, M., Rakowski, W., 2016. Mechanical and tribological properties of carbon-based graded coatings. J. Nanomater. 2016, 1–14. http://dx.doi.org/10.1155/2016/8306345.

Laurent, S., Forge, D., Port, M., Roch, A., Robic, C., Vander Elst, L., Muller, R.N., 2010. Magnetic iron oxide nanoparticles: synthesis, stabilization, vectorization, physicochemical characterizations, and biological applications. Chem. Rev. 110. http://dx.doi.org/10.1021/cr900197g, pp. 2574–2574.

Lee, J.E., Lee, N., Kim, T., Kim, J., Hyeon, T., 2011. Multifunctional mesoporous silica nanocomposite nanoparticles for theranostic applications. Acc. Chem. Res. 44, 893–902. http://dx.doi.org/10.1021/ar2000259.

Lee, S., Choi, S.U.-S., Li, S., Eastman, J.A., 1999. Measuring thermal conductivity of fluids containing oxide nanoparticles. J. Heat Transfer 121, 280–285. http://dx.doi.org/10.1115/1.2825978.

Lei, Y.-M., Huang, W.-X., Zhao, M., Chai, Y.-Q., Yuan, R., Zhuo, Y., 2015. Electrochemiluminescence resonance energy transfer system: mechanism and application in ratiometric aptasensor for lead ion. Anal. Chem. 87, 7787–7794. http://dx.doi.org/10.1021/acs.analchem.5b01445.

Li, D., Baydoun, H., Verani, C.N., Brock, S.L., 2016. Efficient water oxidation using CoMnP nanoparticles. J. Am. Chem. Soc. 138, 4006–4009. http://dx.doi.org/10.1021/jacs.6b01543.

Lin, G., Zhang, Q., Lin, X., Zhao, D., Jia, R., Gao, N., Zuo, Z., Xu, X., Liu, D., 2015. Enhanced photoluminescence of gallium phosphide by surface plasmon resonances of metallic nanoparticles. RSC Adv. 5, 48275–48280. http://dx.doi.org/10.1039/C5RA07368E.

Liu, D., Li, C., Zhou, F., Zhang, T., Zhang, H., Li, X., Duan, G., Cai, W., Li, Y., 2015a. Rapid synthesis of monodisperse Au nanospheres through a laser irradiation -induced shape conversion, self-assembly and their electromagnetic coupling SERS enhancement. Sci. Rep. 5, 7686. http://dx.doi.org/10.1038/srep07686.

Liu, D., Zhou, W., Wu, J., 2016. $CuO\text{-}CeO_2$/ZSM-5 composites for reactive adsorption of hydrogen sulphide at high temperature. Can. J. Chem. Eng. 94, 2276–2281. http://dx.doi.org/10.1002/cjce.22613.

Liu, J., Liu, Y., Liu, N., Han, Y., Zhang, X., Huang, H., Lifshitz, Y., Lee, S.-T., Zhong, J., Kang, Z., 2015b. Metal-free efficient photocatalyst for stable visible water splitting via a two-electron pathway. Science 80 (347), 970–974. http://dx.doi.org/10.1126/science.aaa3145.

Loureiro, A., Azoia, N.G., Gomes, A.C., Cavaco-Paulo, A., 2016. Albumin-based nanodevices as drug carriers. Curr. Pharm. Des. 22, 1371–1390.

Lykhach, Y., Kozlov, S.M., Skála, T., Tovt, A., Stetsovych, V., Tsud, N., Dvořák, F., Johánek, V., Neitzel, A., Mysliveček, J., Fabris, S., Matolín, V., Neyman, K.M., Libuda, J., 2015. Counting electrons on supported nanoparticles. Nat. Mater. http://dx.doi.org/10.1038/nmat4500.

Ma, E., 2003. Nanocrystalline materials: controlling plastic instability. Nat. Mater. 2, 7–8. http://dx.doi.org/10.1038/nmat797.

Ma, S., Livingstone, R., Zhao, B., Lombardi, J.R., 2011. Enhanced Raman spectroscopy of nanostructured semiconductor phonon modes. J. Phys. Chem. Lett. 2, 671–674. http://dx.doi.org/10.1021/jz2001562.

Mabena, L.F., Sinha Ray, S., Mhlanga, S.D., Coville, N.J., 2011. Nitrogen-doped carbon nanotubes as a metal catalyst support. Appl. Nanosci. 1, 67–77. http://dx.doi.org/10.1007/s13204-011-0013-4.

Mallakpour, S., Sirous, F., 2015. Surface coating of α-Al_2O_3 nanoparticles with poly(vinyl alcohol) as biocompatible coupling agent for improving properties of bio-active poly(amide-imide) based nanocomposites having l-phenylalanine linkages. Prog. Org. Coat. 85, 138–145. http://dx.doi.org/10.1016/j.porgcoat.2015.03.021.

Mansha, M., Khan, I., Ullah, N., Qurashi, A., 2017. Synthesis, characterization and visible-light-driven photoelectrochemical hydrogen evolution reaction of carbazole-containing conjugated polymers. Int. J. Hydrogen Energy. http://dx.doi.org/10.1016/j.ijhydene.2017.02.053.

Mansha, M., Qurashi, A., Ullah, N., Bakare, F.O., Khan, I., Yamani, Z.H., 2016. Synthesis of In_2O_3/graphene heterostructure and their hydrogen gas sensing properties. Ceram. Int. 42, 11490–11495. http://dx.doi.org/10.1016/j.ceramint.2016.04.035.

Martis, E., Badve, R., Degwekar, M., 2012. Nanotechnology based devices and applications in medicine: an overview. Chron. Young Sci. 3, 68. http://dx.doi.org/10.4103/2229-5186.94320.

Masciangioli, T., Zhang, W.-X., 2003. Peer reviewed: environmental technologies at the nanoscale. Environ. Sci. Technol. 37, 102A–108A. http://dx.doi.org/10.1021/es0323998.

Mashaghi, S., Jadidi, T., Koenderink, G., Mashaghi, A., 2013. Lipid nanotechnology. Int. J. Mol. Sci. 14, 4242–4282. http://dx.doi.org/10.3390/ijms14024242.

Millstone, J.E., Kavulak, D.F.J., Woo, C.H., Holcombe, T.W., Westling, E.J., Briseno, A.L., Toney, M.F., Fréchet, J.M.J., 2010. Synthesis, properties, and electronic applications of size-controlled poly(3-hexylthiophene) nanoparticles. Langmuir 26, 13056–13061. http://dx.doi.org/10.1021/la1022938.

Mirzadeh, E., Akhbari, K., 2016. Synthesis of nanomaterials with desirable morphologies from metal–organic frameworks for various applications. CrystEngComm 18, 7410–7424. http://dx.doi.org/10.1039/C6CE01076H.

Mogilevsky, G., Hartman, O., Emmons, E.D., Balboa, A., DeCoste, J.B., Schindler, B.J., Iordanov, I., Karwacki, C.J., 2014. Bottom-up

synthesis of anatase nanoparticles with graphene domains. ACS Appl. Mater. Interfaces. 6, 10638–10648. http://dx.doi.org/10.1021/am502322y.

Muehlethaler, C., Leona, M., Lombardi, J.R., 2016. Review of surface enhanced Raman scattering applications in forensic science. Anal. Chem. 88, 152–169. http://dx.doi.org/10.1021/acs.analchem.5b04131.

Mueller, N.C., Nowack, B., 2008. Exposure modeling of engineered nanoparticles in the environment. Environ. Sci. Technol. 42, 4447–4453. http://dx.doi.org/10.1021/es7029637.

Nagarajan, P.K., Subramani, J., Suyambazhahan, S., Sathyamurthy, R., 2014. Nanofluids for solar collector applications: a review. Energy Procedia 61, 2416–2434. http://dx.doi.org/10.1016/j.egypro.2014.12.017.

Navarro, E., Piccapietra, F., Wagner, B., Marconi, F., Kaegi, R., Odzak, N., Sigg, L., Behra, R., 2008. Toxicity of silver nanoparticles to *Chlamydomonas reinhardtii*. Environ. Sci. Technol. 42, 8959–8964. http://dx.doi.org/10.1021/es801785m.

Needham, D., Arslanagic, A., Glud, K., Hervella, P., Karimi, L., Høeilund-Carlsen, P.-F., Kinoshita, K., Mollenhauer, J., Parra, E., Utoft, A., Walke, P., 2016. Bottom up design of nanoparticles for anti-cancer diapeutics: "put the drug in the cancer's food". J. Drug Target. 1–21. http://dx.doi.org/10.1080/1061186X.2016.1238092.

Ngoy, J.M., Wagner, N., Riboldi, L., Bolland, O., 2014. A CO_2 capture technology using multi-walled carbon nanotubes with polyaspartamide surfactant. Energy Procedia 63, 2230–2248. http://dx.doi.org/10.1016/j.egypro.2014.11.242.

Nikalje, A.P., 2015. Nanotechnology and its applications in medicine. Med Chem 5. http://dx.doi.org/10.4172/2161-0444.1000247.

Ning, F., Shao, M., Xu, S., Fu, Y., Zhang, R., Wei, M., Evans, D.G., Duan, X., 2016. TiO_2/graphene/NiFe-layered double hydroxide nanorod array photoanodes for efficient photoelectrochemical water splitting. Energy Environ. Sci. 9, 2633–2643. http://dx.doi.org/10.1039/C6EE01092J.

O'Brien, S., Brus, L., Murray, C.B., 2001. Synthesis of monodisperse nanoparticles of barium titanate: toward a generalized strategy of oxide nanoparticle synthesis. J. Am. Chem. Soc. 123, 12085–12086. http://dx.doi.org/10.1021/ja011414a.

Olteanu, N.L., Lazăr, C.A., Petcu, A.R., Meghea, A., Rogozea, E.A., Mihaly, M., 2016a. "One-pot" synthesis of fluorescent Au@SiO_2 and SiO_2@Au nanoparticles. Arab. J. Chem. 9, 854–864. http://dx.doi.org/10.1016/j.arabjc.2015.12.014.

Olteanu, N.L., Rogozea, E.A., Popescu, S.A., Petcu, A.R., Lazăr, C. A., Meghea, A., Mihaly, M., 2016b. "One-pot" synthesis of Au–ZnO–SiO_2 nanostructures for sunlight photodegradation. J. Mol. Catal. A: Chem. 414, 148–159. http://dx.doi.org/10.1016/j.molcata.2016.01.007.

Oprea, B., Martínez, L., Román, E., Vanea, E., Simon, S., Huttel, Y., 2015. Dispersion and functionalization of nanoparticles synthesized by gas aggregation source: opening new routes toward the fabrication of nanoparticles for biomedicine. Langmuir 31, 13813–13820. http://dx.doi.org/10.1021/acs.langmuir.5b03399.

Pal, M., Pal, U., Jiménez, J.M.G.Y., Pérez-Rodríguez, F., 2012. Effects of crystallization and dopant concentration on the emission behavior of TiO_2: Eu nanophosphors. Nanoscale Res. Lett. 7, 1. http://dx.doi.org/10.1186/1556-276X-7-1.

Pant, H.R., Pant, B., Sharma, R.K., Amarjargal, A., Kim, H.J., Park, C.H., Tijing, L.D., Kim, C.S., 2013. Antibacterial and photocatalytic properties of Ag/TiO_2/ZnO nano-flowers prepared by facile one-pot hydrothermal process. Ceram. Int. 39, 1503–1510. http://dx.doi.org/10.1016/j.ceramint.2012.07.097.

Parveen, K., Banse, V., Ledwani, L., 2016. Green synthesis of nanoparticles: their advantages and disadvantages. Acta Nat., 20048 http://dx.doi.org/10.1063/1.4945168.

Peng, K., Fu, L., Yang, H., Ouyang, J., 2016. Perovskite $LaFeO_3$/-montmorillonite nanocomposites: synthesis, interface characteristics and enhanced photocatalytic activity. Sci. Rep. 6, 19723. http://dx.doi.org/10.1038/srep19723.

Pokhrel, M., Wahid, K., Mao, Y., 2016. Systematic studies on RE_2-Hf_2O_7:5%Eu^{3+} (RE = Y, La, Pr, Gd, Er, and Lu) nanoparticles: effects of the A-site RE^{3+} cation and calcination on structure and photoluminescence. J. Phys. Chem. C 120, 14828–14839. http://dx.doi.org/10.1021/acs.jpcc.6b04798.

Prashant, K.J., Ivan, H.S., 2007. Au NPs target cancer. Nanotoday 2, 19–29.

Priyadarshana, G., Kottegoda, N., Senaratne, A., de Alwis, A., Karunaratne, V., Priyadarshana, G., Kottegoda, N., Senaratne, A., de Alwis, A., Karunaratne, V., 2015. Synthesis of magnetite nanoparticles by top-down approach from a high purity ore. J. Nanomater. 2015, 1–8. http://dx.doi.org/10.1155/2015/317312.

Puri, A., Loomis, K., Smith, B., Lee, J.-H., Yavlovich, A., Heldman, E., Blumenthal, R., 2009. Lipid-based nanoparticles as pharmaceutical drug carriers: from concepts to clinic. Crit. Rev. Ther. Drug Carrier Syst. 26, 523–580.

Qi, M., Zhang, K., Li, S., Wu, J., Pham-Huy, C., Diao, X., Xiao, D., He, H., 2016. Superparamagnetic Fe_3O_4 nanoparticles: synthesis by a solvothermal process and functionalization for a magnetic targeted curcumin delivery system. New J. Chem. 4480, 4480–4491. http://dx.doi.org/10.1039/c5nj02441b.

Qu, Z., Liu, P., Yang, X., Wang, F., Zhang, W., Fei, C., 2016. Microstructure and characteristic of $BiVO_4$ prepared under different pH values: photocatalytic efficiency and antibacterial activity. Materials 9, 129. http://dx.doi.org/10.3390/ma9030129.

Ramacharyulu, P.V.R.K., Muhammad, R., Praveen Kumar, J., Prasad, G.K., Mohanty, P., 2015. Iron phthalocyanine modified mesoporous titania nanoparticles for photocatalytic activity and CO_2 capture applications. Phys. Chem. Chem. Phys. 17, 26456–26462. http://dx.doi.org/10.1039/C5CP03576G.

Rao, J.P., Geckeler, K.E., 2011. Polymer nanoparticles: preparation techniques and size-control parameters. Prog. Polym. Sci. 36, 887–913. http://dx.doi.org/10.1016/j.progpolymsci.2011.01.001.

Rawal, I., Kaur, A., 2013. Synthesis of mesoporous polypyrrole nanowires/nanoparticles for ammonia gas sensing application. Sens. Actuators A Phys. 203, 92–102. http://dx.doi.org/10.1016/j.sna.2013.08.023.

Rawat, M.K., Jain, A., Singh, S., Mehnert, W., Thunemann, A.F., Souto, E.B., Mehta, A., Vyas, S.P., 2011. Studies on binary lipid matrix based solid lipid nanoparticles of repaglinide: in vitro and in vivo evaluation. J. Pharm. Sci. 100, 2366–2378. http://dx.doi.org/10.1002/jps.22435.

Reiss, G., Hütten, A., 2005. Magnetic nanoparticles: applications beyond data storage. Nat. Mater. 4, 725–726. http://dx.doi.org/10.1038/nmat1494.

Feynman, Richard P., 1960. There's plenty of room at the bottom. Eng. Sci. 22, 22–36.

Ripp, S., Henry, T.B. (Eds.), 2011. Biotechnology and Nanotechnology Risk Assessment: Minding and Managing the Potential Threats around Us, ACS Symposium Series. American Chemical Society, Washington, DC, DC. http://dx.doi.org/10.1021/bk-2011-1079.

Rogozea, E.A., Olteanu, N.L., Petcu, A.R., Lazar, C.A., Meghea, A., Mihaly, M., 2016. Extension of optical properties of ZnO/SiO_2 materials induced by incorporation of Au or NiO nanoparticles. Opt. Mater. 56, 45–48. http://dx.doi.org/10.1016/j.optmat.2015.12.020.

Rogozea, E.A., Petcu, A.R., Olteanu, N.L., Lazar, C.A., Cadar, D., Mihaly, M., 2017. Tandem adsorption-photodegradation activity induced by light on NiO-ZnO p–n couple modified silica nanomaterials. Mater. Sci. Semicond. Process. 57, 1–11. http://dx.doi.org/10.1016/j.mssp.2016.10.006.

Saeed, K., Khan, I., 2016. Preparation and characterization of single-walled carbon nanotube/nylon 6,6 nanocomposites. Instrum Sci. Technol. 44, 435–444. http://dx.doi.org/10.1080/10739149.2015.1127256.

Saeed, K., Khan, I., 2014. Preparation and properties of single-walled carbon nanotubes/poly(butylene terephthalate) nanocomposites.

Iran. Polym. J. 23, 53–58. http://dx.doi.org/10.1007/s13726-013-0199-2.

Sagadevan, S., 2015. A review on role of nanofluids for solar energy applications, vol. 3, p. 53. <http://www.sciencepublishinggroup.com>, http://dx.doi.org/10.11648/J.NANO.20150303.14.

Shaalan, M., Saleh, M., El-Mahdy, M., El-Matbouli, M., 2016. Recent progress in applications of nanoparticles in fish medicine: a review. Nanomed. Nanotechnol. Biol. Med. 12, 701–710. http://dx.doi.org/10.1016/j.nano.2015.11.005.

Shao, W., Nabb, D., Renevier, N., Sherrington, I., Luo, J.K., 2012. Mechanical and corrosion resistance properties of TiO_2 nanoparticles reinforced Ni coating by electrodeposition. IOP Conf. Ser. Mater. Sci. Eng. 40, 12043. http://dx.doi.org/10.1088/1757-899X/40/1/012043.

Shin, W.-K., Cho, J., Kannan, A.G., Lee, Y.-S., Kim, D.-W., 2016. Cross-linked composite gel polymer electrolyte using mesoporous methacrylate-functionalized SiO_2 nanoparticles for lithium-ion polymer batteries. Sci. Rep. 6, 26332. http://dx.doi.org/10.1038/srep26332.

Sigmund, W., Yuh, J., Park, H., Maneeratana, V., Pyrgiotakis, G., Daga, A., Taylor, J., Nino, J.C., 2006. Processing and structure relationships in electrospinning of ceramic fiber systems. J. Am. Ceram. Soc. 89, 395–407. http://dx.doi.org/10.1111/j.1551-2916.2005.00807.x.

Sikora, A., Shard, A.G., Minelli, C., 2016. Size and ζ-potential measurement of silica nanoparticles in serum using tunable resistive pulse sensing. Langmuir 32, 2216–2224. http://dx.doi.org/10.1021/acs.langmuir.5b04160.

Sun, S., 2000. Monodisperse FePt nanoparticles and ferromagnetic FePt nanocrystal superlattices. Science 80 (287), 1989–1992. http://dx.doi.org/10.1126/science.287.5460.1989.

Swadeshmukul, S., Peng, Z., Kemin, W., Rovelyn, T., Weihong, T., 2001. Conjugation of biomolecules with luminophore-doped silica nanoparticles for photostable biomarkers. Anal. Chem. 73, 4988–4993. http://dx.doi.org/10.1021/AC010406+.

Swinehart, D.F., 1962. The Beer-Lambert law. J. Chem. Educ. 39, 333. http://dx.doi.org/10.1021/ed039p333.

Thomas, S., Harshita, B.S.P., Mishra, P., Talegaonkar, S., 2015. Ceramic nanoparticles: fabrication methods and applications in drug delivery. Curr. Pharm. Des. 21, 6165–6188. http://dx.doi.org/10.2174/1381612821666151027153246.

Tiwari, J.N., Tiwari, R.N., Kim, K.S., 2012. Zero-dimensional, one-dimensional, two-dimensional and three-dimensional nanostructured materials for advanced electrochemical energy devices. Prog. Mater Sci. 57, 724–803. http://dx.doi.org/10.1016/j.pmatsci.2011.08.003.

Todescato, F., Fortunati, I., Minotto, A., Signorini, R., Jasieniak, J., Bozio, R., 2016. Engineering of semiconductor nanocrystals for light emitting applications. Materials 9, 672. http://dx.doi.org/10.3390/ma9080672.

Torchynska, T.V., El Filali, B., Ballardo Rodríguez, I.C., Shcherbyna, L., 2016. Defect related emission of ZnO and ZnO Cu nanocrystals prepared by electrochemical method. Phys. Status Solidi 13, 594–597. http://dx.doi.org/10.1002/pssc.201510277.

Tratnyek, P.G., Johnson, R.L., 2006. Nanotechnologies for environmental cleanup. Nano Today 1, 44–48. http://dx.doi.org/10.1016/S1748-0132(06)70048-2.

Ullah, H., Khan, I., Yamani, Z.H., Qurashi, A., 2017. Sonochemical-driven ultrafast facile synthesis of SnO_2 nanoparticles: growth mechanism structural electrical and hydrogen gas sensing properties. Ultrason. Sonochem. 34, 484–490. http://dx.doi.org/10.1016/j.ultsonch.2016.06.025.

Unser, S., Bruzas, I., He, J., Sagle, L., 2015. Localized surface plasmon resonance biosensing: current challenges and approaches. Sensors 15, 15684–15716. http://dx.doi.org/10.3390/s150715684.

Wan, D., Chen, H.-L., Lin, Y.-S., Chuang, S.-Y., Shieh, J., Chen, S.-H., 2009. Using spectroscopic ellipsometry to characterize and apply the optical constants of hollow gold nanoparticles. ACS Nano 3, 960–970. http://dx.doi.org/10.1021/nn8009008.

Wang, D.-W., Su, D., 2014. Heterogeneous nanocarbon materials for oxygen reduction reaction. Energy Environ. Sci. 7, 576. http://dx.doi.org/10.1039/c3ee43463j.

Wang, J., Yang, N., Tang, H., Dong, Z., Jin, Q., Yang, M., Kisailus, D., Zhao, H., Tang, Z., Wang, D., 2013. Accurate control of multishelled Co_3O_4 hollow microspheres as high-performance anode materials in lithium-ion batteries. Angew. Chemie Int. Ed. 52, 6417–6420. http://dx.doi.org/10.1002/anie.201301622.

Wang, Y.-C., Engelhard, M.H., Baer, D.R., Castner, D.G., 2016. Quantifying the impact of nanoparticle coatings and nonuniformities on XPS analysis: gold/silver core-shell nanoparticles. Anal. Chem. 88, 3917–3925. http://dx.doi.org/10.1021/acs.analchem.6b00100.

Wang, Y., Xia, Y., 2004. Bottom-up and top-down approaches to the synthesis of monodispersed spherical colloids of low melting-point metals. Nano Lett. 4, 2047–2050. http://dx.doi.org/10.1021/nl048689j.

Wang, Z., Pan, X., He, Y., Hu, Y., Gu, H., Wang, Y., Wang, Z., Pan, X., He, Y., Hu, Y., Gu, H., Wang, Y., 2015. Piezoelectric nanowires in energy harvesting applications. Adv. Mater. Sci. Eng. 2015, 1–21. http://dx.doi.org/10.1155/2015/165631.

Weiss, J., Takhistov, P., McClements, D.J., 2006. Functional materials in food nanotechnology. J. Food Sci. 71, R107–R116. http://dx.doi.org/10.1111/j.1750-3841.2006.00195.x.

Wu, W., He, Q., Jiang, C., 2008. Magnetic iron oxide nanoparticles: synthesis and surface functionalization strategies. Nanoscale Res. Lett. 3, 397–415. http://dx.doi.org/10.1007/s11671-008-9174-9.

Xia, T., Kovochich, M., Liong, M., Mädler, L., Gilbert, B., Shi, H., Yeh, J.I., Zink, J.I., Nel, A.E., 2008. Comparison of the mechanism of toxicity of zinc oxide and cerium oxide nanoparticles based on dissolution and oxidative stress properties. ACS Nano 2, 2121–2134. http://dx.doi.org/10.1021/nn800511k.

Yin, Q., Wu, W., Qiao, R., Ke, X., Hu, Y., Li, Z., 2016. Glucose-assisted transformation of Ni-doped-ZnO@carbon to a Ni-doped-ZnO@void@SiO_2 core–shell nanocomposite photocatalyst. RSC Adv. 6, 38653–38661. http://dx.doi.org/10.1039/C5RA26631A.

Young, K.J., Martini, L.A., Milot, R.L., Snoeberger, R.C., Batista, V.S., Schmuttenmaer, C.A., Crabtree, R.H., Brudvig, G.W., 2012. Light-driven water oxidation for solar fuels. Coord. Chem. Rev. http://dx.doi.org/10.1016/j.ccr.2012.03.031.

Yu, Z.B., Xie, Y.P., Liu, G., Lu, G.Q., Ma, X.L., Cheng, H.-M., 2013. Self-assembled CdS/Au/ZnO heterostructure induced by surface polar charges for efficient photocatalytic hydrogen evolution. J. Mater. Chem. A 1, 2773. http://dx.doi.org/10.1039/c3ta01476b.

Zhang, J., Saltzman, M., 2013. Engineering biodegradable nanoparticles for drug and gene delivery. Chem. Eng. Prog. 109, 25–30.

Zhang, X., Lai, Z., Liu, Z., Tan, C., Huang, Y., Li, B., Zhao, M., Xie, L., Huang, W., Zhang, H., 2015. A facile and universal top-down method for preparation of monodisperse transition-metal dichalcogenide nanodots. Angew. Chemie Int. Ed. 54, 5425–5428. http://dx.doi.org/10.1002/anie.201501071.

Zhou, Y., Dong, C.-K., Han, L., Yang, J., Du, X.-W., 2016. Top-down preparation of active cobalt oxide catalyst. ACS Catal. 6, 6699–6703. http://dx.doi.org/10.1021/acscatal.6b02416.

Zhu, Y., Goodridge, a G., Stapleton, S.R., 1994. Zinc, vanadate and selenate inhibit the tri-iodothyronine-induced expression of fatty acid synthase and malic enzyme in chick-embryo hepatocytes in culture. Biochem. J. 303, 213–216.

Zhuang, J., Gentry, R.W., 2011. Environmental application and risks of nanotechnology: a balanced view. pp. 41–67. http://dx.doi.org/10.1021/bk-2011-1079.ch003.